Experimental determination of the $^{17}O(p,\alpha)^{14}N$ and $^{17}O(p,\gamma)^{18}F$ reaction rates

A. Chafa, V. Tatischeff, P. Aguer, S. Barhoumi, A. Coc, F. Garrido, M. Hernanz, J. José, J. Kiener, A. Lefebvre-Schuhl, et al.

Experimental determination of the ^{17}O(p,α)^{14}N and ^{17}O(p,γ)^{18}F reaction rates

A. Chafa,[1] V. Tatischeff,[2] P. Aguer,[3] S. Barhoumi,[4] A. Coc,[2] F. Garrido,[2] M. Hernanz,[5] J. José,[6] J. Kiener,[2] A. Lefebvre-Schuhl,[2] S. Ouichaoui,[1] N. de Séréville,[2,7] and J.-P. Thibaud[2]

[1] *USTHB-Faculté de Physique, BP 32, El-Alia, 16111 Bab Ezzouar, Algiers, Algeria*
[2] *CSNSM, IN2P3-CNRS and Univ Paris-Sud, F-91405 Orsay Cedex, France*
[3] *CENBG, IN2P3-CNRS and Univ Bordeaux I, F-33175 Gradignan, France*
[4] *UMBM, B.P. 166, Route ICHBILLIA, 28000 M'sila, Algeria*
[5] *Institut de Ciències de l'Espai (CSIC), and Institut d'Estudis Espacials de Catalunya, E-08034 Barcelona, Spain*
[6] *Departament de Física i Enginyeria Nuclear (UPC) and Institut d'Estudis Espacials de Catalunya, E-08034 Barcelona, Spain*
[7] *Université Catholique de Louvain, Chemin du Cyclotron 2, B-1348 Louvain-la-Neuve, Belgium*

(Dated: February 20, 2007)

The ^{17}O(p,α)^{14}N and ^{17}O(p,γ)^{18}F reactions are of major importance for hydrogen-burning nucleosynthesis in a number of different stellar sites. In particular, ^{17}O and ^{18}F nucleosynthesis in classical novae is strongly dependent on the thermonuclear rates of these two reactions. The previously estimated rate for ^{17}O(p,α)^{14}N carries very large uncertainties in the temperature range of classical novae (T=0.01–0.4 GK) whereas a recent measurement has reduced the uncertainty of the ^{17}O(p,γ)^{18}F rate. We report on the observation of a previously undiscovered resonance at $E_{\rm c.m.}$=183.3 keV in the ^{17}O(p,α)^{14}N reaction, with a measured resonance strength $\omega\gamma_{p\alpha}$=(1.6±0.2)×10^{-3} eV. We studied in the same experiment the ^{17}O(p,γ)^{18}F reaction by an activation method and the resonance strength was found to amount to $\omega\gamma_{p\gamma}$=(2.2±0.4)×10^{-6} eV. The excitation energy of the corresponding level in ^{18}F was determined to be 5789.8±0.3 keV in a DSAM measurement which yielded a value of τ<2.6 fs for the level lifetime. The ^{17}O(p,α)^{14}N and ^{17}O(p,γ)^{18}F reaction rates were calculated using the measured resonance properties and reconsidering some previous analyses of the contributions of other levels or processes. The ^{17}O(p,α)^{14}N rate is now well established below T=1.5 GK with uncertainties reduced by orders of magnitude in the temperature range T=0.1–0.4 GK. The uncertainty in the ^{17}O(p,γ)^{18}F rate is somewhat larger due to remaining obscurities in the knowledge of the direct capture process. These new resonance properties have important consequences for ^{17}O nucleosynthesis and γ-ray emission of classical novae.

PACS numbers: 26.30.+k, 25.40.Ny, 25.40.Lw, 27.20.+n, 26.50.+x

I. INTRODUCTION

Precise knowledge of the ^{17}O(p,α)^{14}N and ^{17}O(p,γ)^{18}F reaction rates is required for evaluating elemental abundances in a number of hydrogen-burning stellar sites, including red giants, asymptotic giant branch (AGB) stars, massive stars, and classical novae. These two reactions are parts of the carbon-nitrogen-oxygen (CNO) cycles. They are specifically very important for the nucleosynthesis of the rare oxygen isotope ^{17}O. Measurements of the oxygen isotopic abundance ratios ^{16}O/^{17}O and ^{16}O/^{18}O have been performed in several types of red giant stars (see [1] and references therein) and in presolar dust grains which formed in stellar outflows [2]. These data provide important information on nucleosynthesis and mixing processes in red giant and AGB stars, as well as on galactic chemical evolution and the age of the Milky Way [3]. However, the ^{16}O/^{17}O surface abundance ratio in evolved stars of mass $\gtrsim 2.5\ M_\odot$ critically depends on the thermonuclear rates of the reactions ^{17}O(p,α)^{14}N and ^{17}O(p,γ)^{18}F [4].

Classical novae are thought to be a major –if not the dominant– source of ^{17}O in the Galaxy [5, 6]. In addition, they can produce the short-lived radio-isotope ^{18}F ($T_{1/2}$=110 minutes) whose β^+ decay is followed by γ-ray emission from positron-electron annihilation, which could be observed with γ-ray satellites like the INTEGRAL observatory [7]. As the ^{17}O(p,α)^{14}N and ^{17}O(p,γ)^{18}F reactions govern the destruction of ^{17}O and the formation of ^{18}F, their rates are decisive in determining the final abundances of these isotopes [8]. Moreover, they have a small but noticeable effect on the energetics of the nova explosion [9].

Stellar temperatures of primary importance for nucleosynthesis are typically in the ranges T=0.01–0.1 GK for red giant, AGB and massive stars, and T=0.01–0.4 GK for classical nova explosions (peak temperatures of 0.35 GK can be easily achieved in explosions hosting very massive white dwarfs). Thus, for classical nova studies, the ^{17}O(p,α)^{14}N and ^{17}O(p,γ)^{18}F reaction cross sections have to be precisely known in the center-of-mass energy range $E_{\rm c.m.}$=0.017–0.37 MeV. In the NACRE compilation of thermonuclear reaction rates [10], the uncertainty in the rate of the ^{17}O(p,α)^{14}N reaction was very important (orders of magnitude) in the temperature range T=0.1–0.4 GK, due to an unobserved narrow resonance at $E_{\rm c.m.}$∼180 keV whose contribution to the total ^{17}O(p,α)^{14}N rate had to be roughly estimated using a limit for the proton partial width [10]. The corresponding resonance in the (p,γ) channel was observed for the first time by Fox et al. [9] during the course of our study. The measured strength of (1.2±0.2)×10^{-6} eV [9, 11] reduces the uncertainty in the ^{17}O(p,γ)^{18}F reaction rate by as much as orders of magnitude at nova temperatures.

The ^{17}O(p,α)^{14}N and ^{17}O(p,γ)^{18}F resonances at $E_{\rm c.m.}$∼180 keV correspond to a level of spin-parity J^π=2$^-$ in ^{18}F, which was previously observed at an excitation energy E_x=5786±2.4 keV via the ^{14}N(α,γ)^{18}F reaction [12, 13]. As reported in Ref. [12], the lifetime of this state was measured to be τ=15±10 fs using the Doppler-shift attenuation method (DSAM). This value implies a somewhat surprising ratio $\Gamma_\gamma/\Gamma_\alpha$∼1. It served to estimate the ^{17}O(p,α)^{14}N resonance strength [10] which came out to be necessarily very small in relation with the small measured total width of the level.

The aim of this study was to measure all the properties of the level of ^{18}F at E_x=5.79 MeV needed for a detailed knowledge of the ^{17}O(p,α)^{14}N and ^{17}O(p,γ)^{18}F reaction rates at nova temperatures. This includes precise determination of the excitation energy, the lifetime and the three partial widths (Γ_p, Γ_γ, Γ_α) of this level through measurement of the resonance strengths in the (p,α) and (p,γ) channels.

A preliminary report on the present work has been given elsewhere [14, 15] and this paper is essentially a detailed version of the previous ones, with special emphasis put on calculation of the reaction rates and on some experimental points which needed to be clarified.

The experimental procedures and results are presented in Sec. II. Sec. II-A describes the DSAM experiment performed to measure both the excitation energy and the lifetime of the J^π=2$^-$ level at 5.79 MeV in ^{18}F. The observation of the previously unknown resonance corresponding to this level in the ^{17}O(p,α)^{14}N reaction is presented in Sec. II-B where the measurement of its strength is described. In Sec. II-C, we report on the determination of the strength of the resonance at the same energy in the (p,γ) channel, using an activation method. Sec. III is devoted to calculations of the reaction rates derived from our measurements. In this section are also discussed revaluations of the contributions coming from other levels or processes. Finally, a summary and conclusions are given in Sec. IV.

II. EXPERIMENTAL PROCEDURES AND RESULTS

A. Excitation energy and lifetime of the J$^\pi$=2$^-$ level at 5790 keV in ^{18}F

The excitation energy and lifetime of the J^π=2$^-$ level at 5790 keV in ^{18}F have been reinvestigated using the Doppler Shift Attenuation Method (DSAM) applied to the ^{14}N(α,γ)^{18}F reaction at $E_\alpha^{\rm lab}$=1775 keV. The corresponding resonance is known to be fairly strong [12, 13] and to lead to relatively simple γ-ray spectra with unidirectional and monoenergetic recoil nuclei.

As already indicated, before this study, the level excitation energy was given as E_x=5786±2.4 keV and its lifetime was found to be 15±10 fs [12]. Such a short lifetime is close to the sensitivity limit of DSAM. Thus, small differences in the measured Doppler shifts can lead to variations of orders of magnitude in the extracted lifetime and consequently in the derived level partial widths and resonance strengths. Furthermore, besides a smaller uncertainty in the calculated rates, a better precision on E_x was helpful in the search of the (p,γ) and (p,α) resonances associated with the considered level.

1. Experimental set-up

Alpha beams of energy in the range E_α=1620-1775 keV were supplied by the 4 MV Van De Graaff accelerator of the CENBG laboratory (Bordeaux). Typical beam intensities on target were 20-30 μA with a 3 mm×3 mm spot. The beam settings were adjusted to furnish parallel trajectories for incoming α-particles in order to improve the angle definition of the emitted γ rays.

The three used TiN targets were fabricated at the CENBG laboratory by nitration in an atmosphere of purified nitrogen of a titanium layer evaporated on a thick copper backing. The TiN layer was made thick enough (∼200 μg cm^{-2}) to allow the simultaneous excitation of at least two of the four resonant levels in ^{18}F between 5.6 and 5.8 MeV excitation energy [13]. The water-cooled targets were placed at 90° relative to the beam direction. A liquid nitrogen trap was placed near the target to reduce carbon accumulation.

The γ rays were detected with three large volume high-purity Ge (HPGe) detectors placed in the horizontal plane at a distance of 9 cm from the target. They were located at the laboratory angles $\theta_{\rm lab}$=0°, 123° and 144°. The three angles were measured with an estimated precision of ±2° by means of optical sightings through a theodolite. The spread in angle due to the finite size of the detectors was estimated from the knowledge of their geometry as given by manufacturers. The efficiencies of the detectors were typically 70% at 1332 keV compared to a standard 3"×3" NaI detector. Their resolution (FWHM) was typically 2.3 keV at the same γ-ray energy. The Ge detector placed at 0° was actively shielded with Bismuth Germanate (BGO) scintillation counters for Compton suppression in a standard geometry [16]. Compton-suppression BGO shields were not installed at 123° and 144° in order to place the Ge detectors as close as possible to the target to keep reasonable γ-ray efficiencies. During the measurements, three radioactive sources of ^{137}Cs, ^{60}Co and ^{88}Y were placed near the target to detect standard calibration lines together with the beam-induced γ rays.

Conventional electronics was used and γ-ray spectra were recorded with a standard acquisition system operating in singles mode.

2. Data analysis tools

Gamma-ray spectra were analyzed using the least-squares peak-fitting program gf3 especially designed by D.C. Radford [17] for use with Germanium detectors. Two components were included in all peaks, namely a Gaussian and a low-energy skewed Gaussian. The dependence on energy of the two parameters defining the shape of the peaks (relative height of the two Gaussians and distance between them) was determined from analysis of a few well-resolved strong lines. The two parameters were then kept fixed to the calculated values in the peak-fitting procedure.

A specific program was written to extract the lifetime and excitation energy of the 5790 keV level from the measured energies of the corresponding lines in the 0°, 123° and 144° spectra. Using Monte Carlo techniques, the energy distribution of the studied Doppler-broadened lines is calculated as a function of lifetime for γ rays detected at a given angle. The distribution of recoil-nucleus velocities is determined as a function of time using the most recent stopping-power data given in Ref. [18]. These data include electronic as well as nuclear stopping powers. The stopping material was considered to be titanium nitride (stoichiometry TiN). Angular scattering of recoiling ions is calculated in the same way, allowing for an investigation of correlation between energy and angular scattering which are usually treated as independent processes [19]. This correlation was found negligible (mean effect of less than 1%) in the specific studied case of short lifetimes where electronic stopping is by far the dominant process. Finally, the program gives a simulation of spectra detected in real detectors, in convoluting the theoretical energy distributions with Gaussian response functions of appropriate variance. The finite size of the γ-ray detectors is taken into account by Monte Carlo techniques. Namely, corrections for efficiency and for angular distribution [12, 20] of the emitted γ rays in the detection cones were evaluated from GEANT [21] for the specific used detectors. Relativistic effects including aberration corrections [22] were fully taken into account in calculating the Doppler-shifted γ-ray energy distribution.

In the present study, the calculated line shapes were not analyzed due to the expected short values of the investigated lifetimes. Instead, we used the first moment of the simulated γ-ray energy distributions.

3. Data analysis and results

Since high-precision energy measurements were needed in that experiment, special care was taken to eliminate the electronic drifts of the system. In each run of typically 20 hours duration, γ-ray spectra were systematically recorded once every hour to allow for subsequent gain adjustment through the code gf3. It was checked after this adjustment that the energy resolution of peaks in the total accumulation was the same as in the short-time partial spectra. Furthermore, four independent measurements were carried out in order to check the overall consistency of the results extracted from the redundant couples of detectors 0°-123° and 0°-144° before extracting the final average values.

The 5790 keV level of ^{18}F was excited at the α-particle bombarding energy $E_\alpha^{\rm lab}$=1775 keV. Thanks to the appropriate target thickness, the level at 5671.6 keV was simultaneously populated to allow for measurements of energy differences relative to this reference peak whose short lifetime (total width Γ=0.13±0.05 keV) [23] ensures fully Doppler-shifted lines. Three runs were carried out in these conditions, using fresh targets for each run, and analysed independently. In addition, a run was performed at $E_\alpha^{\rm lab}$=1623 keV to excite simultaneously the 5672 keV level and the reference levels at 5603–5605 keV [13], in order to check the previously determined excitation energy of the 5672 keV level [24].

A section of a typical γ-ray spectrum taken at $\theta_{\rm lab}$=0° and $E_\alpha^{\rm lab}$=1775 keV is shown in Fig. 1. The lines used for calibration are indicated together with the resonant γ rays of interest. Figure 2 presents a relevant section of this spectrum where show up the full-energy (FE) lines R→1081 keV and R→937 keV for the resonant level at 5790 keV (the precise excitation energies of the final states are 1080.54±0.12 and 937.20±0.06 keV, respectively [13]).

In the analysis of the spectra, two separate energy calibrations were used. The first one, corresponding to the low-energy part of the spectra (E_γ<4.2 MeV), was based on lines from standard sources (^{137}Cs, ^{60}Co and ^{88}Y) and from the ^{40}K natural radioactivity. In addition, we took advantage of boron contamination in the target to include in the set of calibration lines the 3853.807→0 keV and 3683.921→0 keV transitions [25] from the ^{10}B(α,p)^{13}C reaction. We checked that the centroids of the corresponding peaks, fitted with the detector response function, are not significantly affected by Doppler shift due to the long lifetime of the 3854 keV level, i.e. τ=8.6 ps [25]. For the 3684→0 keV transition, two distinct components can be identified on the spectra (see Fig. 1): a narrow one coming from the feeding of the 3684 keV level by a transition from the long-lived 3854 keV level and a broad one which is from transitions implying shorter-lived levels. Only the slow component of this line was considered for the energy calibration. Centroid values obtained from the fitting process were used to determine the quadratic energy calibration. Observed χ^2 values for the best estimated parameters lead to an energy uncertainty of ±200 eV at the three angles. The low-energy calibration served in determining the energies of the following transitions: 5672→3134 keV (FE), 5672→3062 keV (FE) and 5672→1081 keV (single escape).

A separate energy calibration was determined for the high-energy part (>4.2 MeV) of the spectra, using the same lines from ^{10}B(α,p)^{13}C and the 5672→1081 keV (FE) and 5672→0 keV (FE) lines. For the latter transitions, the excitation energy of the 5672 keV level deduced

from the low-energy part of the spectra (see below) was used. The involved full Doppler shifts were calculated from the Monte Carlo code taking into account the finite size of the detectors at the various angles as indicated above. A quadratic calibration was also used. The absolute energy uncertainty was larger than in the low-energy case due to the necessary introduction of Doppler-shifted reference lines. It was estimated to ±220 eV at $\theta_{\rm lab}$=0° and ±280 eV at backward angles. The high-energy calibration served to measure the shifted energies of the 5790→1081 keV (FE) and 5790→937 keV (FE) transitions.

In order to reduce the final uncertainty in the 5790 keV level, the Doppler-shifted energies of the corresponding γ-ray lines were measured relative to those deexciting the level at 5672 keV. We first did a new measurement of the excitation energy of the level at 5672 keV, given as 5672.57±0.32 keV in a previous experiment [24]. For this study, we analysed the spectra taken at $\theta_{\rm lab}$=0° in two runs at $E_\alpha^{\rm lab}$=1775 keV (using two different targets) and a third one at $E_\alpha^{\rm lab}$=1623 keV (see above). As already mentioned, the lifetime of the studied level is known to be very short, which ensures full Doppler shifts for the measured transitions R→3134 keV, R→3061 keV and R→1081 keV. For the transition R→3134 keV, the peak-fitting procedure had to take into account a doublet including a low-intensity component of close energy (∼4 keV) corresponding to the transition 5603→3062 keV.

Nine compatible results were obtained from analysis of the three lines in the three independent measurements. We finally obtained the weighted mean value of E_x=5671.6±0.2 keV for the considered level. This result is ∼1 keV less than the previous value obtained in Ref. [24]. The discrepancy could be due to the erroneous value of 3853.807 keV adopted by the authors for the energy of the calibration line from the ^{10}B(α,p)^{13}C reaction, instead of the correct one: 3853.170±0.022 keV.

The excitation energy and lifetime of the 5790 keV level were determined from the measurements of the differences in energy of the two lines 5790→1081 keV and 5790→937 keV and of the adjacent line corresponding to the transition 5672→1081 keV. These energy differences, Δ_i, were measured for the three detection angles θ_i=0°, 123° and 144° from analysis of spectra similar to the one shown in Fig. 2. For levels with comparable lifetimes, such a relative measurement has the advantage to strongly reduce the effect of the uncertainty in the angular position of the Ge detectors, because in this case the angular dependence is only effective on the difference in the Doppler shifts of the studied and the reference lines.

The results obtained for the 5790→1081 keV transition are shown in Fig. 3 for the couple of angles θ_0=0°, θ_1=123°. In this figure, we compare in the Δ_0–Δ_1 plane the measured value and the calculations from the Monte Carlo program described above. The experimental value is given together with the covariance ellipse corresponding to the bivariate normal distribution of the two independent random variables Δ_0 and Δ_1. The standard deviations of Δ_0 and Δ_1 are 0.3 keV and 0.4 keV, respectively. The calculated energy differences are given by a step of 2 fs in the lifetime range 0–22 fs for three excitation energy values of the resonant level, namely 5789.5, 5789.8 and 5790.1 keV. The effect of the uncertainties in the angular position of the detectors is negligible : when assuming a largely overestimated error of 5° on the angle θ_1=123°, the corresponding error on Δ_1 is found to be less than 0.1 keV in the whole lifetime range 0–30 fs, i.e. well below the uncertainty arising from centroid determination and energy calibration. The result extracted from Fig. 3 is E_x=5789.84±0.27 keV and $\tau\leq$5.1 fs (here the error bar on E_x does not take into account the uncertainty in the energy of the reference line).

From plots similar to the one shown in Fig. 3, four consistent couples of values "Excitation energy–lifetime" were obtained from analysis of the two transitions 5790→1081 keV and 5790→937 keV. Taking into account the partial correlation between the two results obtained for the same transition (0°–123° and 0°–144°) due to the unique measured value Δ_0, the weighted average amounts to E_x=5789.8±0.3 keV and $\tau\leq$2.6 fs (85% confidence level).

The error bar of E_x takes into account the uncertainty in the energy of the reference level at 5671.6±0.2 keV. In view of the very short value observed for τ, the uncertainty arising from stopping power values has not been considered. The excitation energy is found to be in good agreement with the very recent result E_x=5788.9±1.0 keV given in Ref. [11] from a study of the ^{17}O(p,γ)^{18}F reaction at $E_{\rm c.m.}$=183 keV. The lifetime value is in disagreement with the previous result τ=15±10 fs of Ref. [12].

B. The $E_{\rm c.m.}$=183.3 keV resonance in the ^{17}O(p,α)^{14}N reaction

The search for the previously unobserved resonance at $E_{\rm c.m.}$=183.3 keV in the ^{17}O(p,α)^{14}N reaction was prompted by the large width (Γ>0.25 eV) found for the corresponding resonant state at E_x=5789.8 keV in ^{18}F. The value of $E_{\rm c.m.}$=183.3±0.6 keV for the resonance energy is calculated from our measured value of the excitation energy of the resonant level and from the Q-value for ^{17}O+p→^{18}F given in Ref. [26], Q=5606.5±0.5 keV. Note that the relatively large error on the resonance energy is essentially due to the uncertainty of 0.5 keV in the Q-value [26].

1. *Targets and apparatus*

The experiment was carried out at the electrostatic accelerator PAPAP of the CSNSM laboratory (Orsay), which can supply intense proton beams of energy E_p<240 keV. The beam energy spread was typically

0.2 keV. More detailed characteristics of the accelerator can be found in Ref. [27]. Beam currents of 60-90 μA were typically sustained on targets. An annular electrode biased at a voltage of -300 V was mounted in front of the target to suppress the escape of secondary electrons.

Targets of tantalum oxide were used in the study of the ^{17}O(p,α)^{14}N reaction. They were fabricated by ^{17}O ion implantation in 0.3 mm thick Ta foils at the SIDONIE implanter of the CSNSM. The total irradiation fluence was 1.5×10^{18} atoms cm^{-2}, equally distributed at 30, 10, and 2.5 keV implantation energies. The resulting target thickness of a few keV is much larger than the width of the level at 5790 keV (Γ=6.8±3 eV, see Sec. III-A). Similar targets enriched in ^{18}O were produced using exactly the same experimental procedure in order to measure the strength of the ^{17}O(p,α)^{14}N resonance relative to that of the well-known resonance at $E_R^{\rm lab}$=150.9 keV in the ^{18}O(p,α)^{15}N reaction (see below).

The targets were placed at 45° with respect to the beam direction and cooled with deionized water. The target holder was surrounded with a copper assembly cooled with liquid nitrogen to limit the carbon build-up during the irradiation. No change in the target stoichiometry was noted from Rutherford backscattering spectrometry (RBS) measurements systematically performed before and after the proton irradiation, where the charge accumulated on each target was typically 1 C. The RBS measurements were performed on both ^{17}O and ^{18}O targets at the ARAMIS accelerator (CSNSM) with ^{4}He beams of 1.2 MeV energy.

In the PAPAP experiment, the outgoing α-particles were detected with 4 passivated implanted planar silicon detectors with active areas of 3 cm^2. They had an energy resolution of 20 keV with a ^{241}Am radioactive source. They were placed at a distance of 14 cm from the target and at laboratory angles of 105°, 120°, 135° and 150°. Each detector was shielded by a 2 μm thick foil of aluminized Mylar in order to stop the intense flux of elastically scattered protons. Detector solid angles were measured with two different calibrated sources: ^{241}Am and a mixed source composed of ^{239}Pu, ^{241}Am and ^{244}Cm. Solid angle values around 1.42×10^{-2} sr were found from these consistent measurements with a typical uncertainty of $\pm0.04\times10^{-2}$ sr.

Standard electronics was used and α-particle spectra were recorded with a data acquisition system operating in singles mode for subsequent analysis.

2. Results

We show in Fig. 4 an α-particle spectrum measured at $E_p^{\rm lab}$=196.5 keV with the detector at θ_{lab}=150°. The strong peak at $E_\alpha\sim$430 keV is due to the previously unobserved resonance at $E_{\rm c.m.}$=183.3 keV in the ^{17}O(p,α)^{14}N reaction. The energy $E_\alpha\sim$430 keV corresponds to that expected for α-decay from the level at 5.7898 MeV to the ground state of ^{14}N when taking into account both α emission at 150° and energy loss in 2 μm thick foils of aluminized Mylar. The broad peak around 3.4 MeV in Fig. 4 originates from the reaction ^{11}B(p,α)2^{4}He due to a slight boron contamination of the targets.

Figure 4b shows the interesting part of the α-spectrum measured at E_p^{lab}=196.5 keV. Alpha-peak intensities were derived from least-squares fits to the data assuming a Gaussian shape with intensity, position and standard deviation as free parameters. Such a fit is shown by the dashed line in Fig. 4b. Dead-time was systematically measured and controlled during the experiment and the small corresponding corrections (<3%) were applied to the derived number of counts.

The α-particle angular distribution was measured for the ^{17}O(p,α)^{14}N resonance at $E_{\rm c.m.}$=183.3 keV. Before this measurement, we checked that the α-particle angular distribution for the ^{18}O(p,α)^{15}N resonance at $E_R^{\rm lab}$=150.9 keV was isotropic, as expected. The results for the ^{17}O(p,α)^{14}N resonance are shown in Fig. 5. The solid line is a Legendre-polynomial fit to the data:

$$W_{\rm c.m.}(\theta_\alpha) = 1 + a_2 P_2(\cos\theta_\alpha) \ , \qquad (1)$$

which yields a_2=0.16±0.03. Note that the Legendre-polynomial development was limited to a_2 since the capture of relative angular momentum l=3 should be weak relative to that of l=1 due to the low energy of the resonance. The adopted development for $W_{\rm c.m.}(\theta_\alpha)$ is thus expected to provide a sufficient description of the angular distribution for the determination of the resonance strength.

The measured excitation function of the ^{17}O(p,α)^{14}N reaction is shown in Fig. 6a. The typical energy step was 0.2 keV and the accumulated charge was 0.04 C per data point. Small corrections were applied on energy to account for a moderate carbon deposit on the target (∼20 eV per point). These corrections were only noticeable for the last measured data points where the carbon build-up was maximal. Alpha yields were also slightly altered by the carbon deposit due to the induced energy straggling. Corrections for this effect were evaluated by measuring excitation functions with targets already used in previous measurement. The resulting corrections were applied to the data points and found to be small (a maximum value of 10% at the end of the measurement and of 1–3% for the most important data points). The given yields result from the sum of the individual values measured at each of the four angles normalized according to the determined angular distribution. We checked that the observed depth profile (Fig. 6a) is consistent with the characteristics (fluences and successive energies) of the implantation procedure. Measurements were repeated with three ^{17}O implanted targets and fully compatible results were obtained.

As already mentioned, the strength of the ^{17}O(p,α)^{14}N resonance was determined relative to that of the strong resonance at $E_R^{\rm lab}$=150.9 keV in the ^{18}O(p,α)^{15}N reaction. Two runs with fresh ^{18}O targets were performed in

between the three ^{17}O ones. They also gave fully compatible results. RBS measurements (see above) performed on ^{17}O and ^{18}O targets showed no difference between the ^{17}O- and ^{18}O-implanted ones. In particular, a similar stoichiometry was found for the ^{17}O and ^{18}O targets whatever the depth and surface position, with a maximum ratio $(\mathrm{O/Ta})_{\max}$=3.1±0.3.

The similarity of the ^{17}O- and ^{18}O-implanted targets is further demonstrated in Fig. 6b which shows a comparison of measured excitation functions for the new resonance at E_R^{lab}=194.1 keV in the ^{17}O$(p,\alpha)^{14}$N reaction and for the 150.9 keV resonance of ^{18}O$(p,\alpha)^{15}$N. The data for the latter resonance were appropriately normalized and shifted in energy to be compared with those obtained with the ^{17}O target. The shift in energy for the data points of the ^{18}O$(p,\alpha)^{15}$N resonance was achieved according to the relation

$$E_{18}\ (\mathrm{keV}) = 194.1 + (E_{18}^{\mathrm{mes}} - 150.9) \times 0.95\ , \quad (2)$$

where the factor 0.95 is the ratio of stopping powers of the ^{17}O and ^{18}O targets for protons of the appropriate energy.

The strength of the ^{17}O$(p,\alpha)^{14}$N resonance was obtained from the relation[1]

$$\omega\gamma_{p\alpha} = \omega\gamma_{p\alpha}^{18}\left(\frac{M_{17}}{M_{17}+m_p}\frac{M_{18}+m_p}{M_{18}}\right)^3 \frac{E_R^{17}}{E_R^{18}}\frac{\epsilon_{17}}{\epsilon_{18}}\frac{Y_{p\alpha}^{17}}{Y_{p\alpha}^{18}}\ . \quad (3)$$

Here, $\omega\gamma_{p\alpha}^{18}$ is the strength of the ^{18}O$(p,\alpha)^{15}$N resonance; m_p, M_{17} and M_{18} are the proton, ^{17}O and ^{18}O masses, respectively; E_R^{17} and E_R^{18} are the laboratory energies of the two resonances; $(\epsilon_{17}/\epsilon_{18})$=0.95±0.05 is the ratio of the effective stopping-powers in the laboratory system [18], where the error arises from the uncertainty in the stoichiometry of the ^{17}O and ^{18}O targets; and $(Y_{p\alpha}^{17}/Y_{p\alpha}^{18})$ is the ratio of the measured reaction yields for the two resonances, which was obtained from the plateau of the excitation functions measured with the ^{17}O and ^{18}O targets (energy range of E_p^{lab}=195.2–196.5 keV in Fig. 6b). This ratio was found to be $(Y_{p\alpha}^{17}/Y_{p\alpha}^{18})=(7.7\pm0.9)\times10^{-3}$, where the major contributions to the uncertainty come from the target composition (10%) and the beam current integration (5%). The strength of the reference resonance at 150.9 keV in the ^{18}O$(p,\alpha)^{15}$N reaction was taken as $\omega\gamma_{p\alpha}^{18}$=0.167±0.012 eV. This value, obtained in a careful measurement by Becker *et al.* [28], is in very good agreement with a previous measurement [29] which gave $\omega\gamma_{p\alpha}^{18}$=0.17±0.02 eV.

We finally obtain $\omega\gamma_{p\alpha}=(1.6\pm0.2)\times10^{-3}$ eV for the strength of the resonance at E_R^{lab}=194.1 keV in the ^{17}O$(p,\alpha)^{14}$N reaction. The main contributions to the error bar have been given above. The statistical uncertainty in the number of counts was negligible as well as the uncertainty in the energies of the two involved resonances.

Our resonance strength value is in very good agreement with the results of two very recent experiments performed either in inverse kinematics [30] or using a different type of ^{17}O target (not implanted) [31].

The resonance energy derived from the measured excitation function was found to be E_R^{lab}=194.3±0.7 keV. To obtain this value, the energy at half the maximum yield was corrected for taking into account the mean implantation depth of the ^{17}O ions at the lowest of the three used energies (see Sec. II-B-1). It is in excellent agreement with the value of 194.1±0.6 keV obtained from the excitation energy of the resonant level and the Q-value for ^{17}O+$p\rightarrow{}^{18}$F.

C. The $E_{\mathrm{c.m.}}$=183.3 keV resonance in the ^{17}O$(p,\gamma)^{18}$F reaction

The strength of the ^{17}O$(p,\gamma)^{18}$F resonance at E_R^{lab}=194.1 keV was obtained from measurements by an activation method of the ^{18}F total production in irradiated ^{17}O targets. The number of produced ^{18}F nuclei was determined from measurement of the 511 keV γ-rays due to β^+ annihilation following ^{18}F radioactive decay. The strength was measured relative to that of the resonance at the same energy in the ^{17}O$(p,\alpha)^{14}$N channel (see above) by measuring the corresponding α-yields during the irradiation phase of the experiment.

1. *Experimental set-up and targets*

The experiment was carried out at the electrostatic accelerator PAPAP of the CSNSM laboratory. The experimental apparatus was exactly the same as described for the ^{17}O$(p,\alpha)^{14}$N experiment, except for γ-ray measurements. The ^{18}F β^+ activity was measured with two large volume HPGe detectors (of 70% efficiency) positioned opposite one another in a very close geometry, in order to register in time coincidence the two 511 keV photons from positron-electron annihilation. A standard fast-slow coincidence system was used for the measurements. The time resolution as measured from the recorded time spectrum was typically 5 ns (FWHM). The events were recorded in a multidimensional data acquisition system for subsequent analysis. The stability of the whole electronics was systematically checked with a special emphasis put on the stability of the contours in the E_γ–E_γ plane used to derive the number of 511–511 keV coincident events.

Targets enriched in ^{17}O were produced by ion implantation in the same conditions as those for the ^{17}O$(p,\alpha)^{14}$N reaction. After irradiation by protons at E_p^{lab}=196.5 keV (on resonance) or E_p^{lab}=192.7 keV (off

[1] Note that there is a typographical error in Eq. (1) of Ref. [14], as the exponent of 3 of the mass ratio term is missing. However, the ^{17}O$(p,\alpha)^{14}$N resonance strength was deduced from the correct equation given here.

resonance), the ^{17}O targets were rapidly (in ∼4 minutes) placed between the two Ge detectors for γ-ray counting. Alpha-particle yields were measured using the same α-detector arrangement as described in Sec. II-B-1.

2. Experimental procedure and results

The ^{17}O-implanted targets were bombarded for typically 5 hours (∼2.7 half-lives of the radioisotope ^{18}F, $T_{1/2}$=109.77 minutes) at ∼70 μA beam intensity. During the target irradiation, α-particle spectra were recorded every 15 minutes together with the corresponding beam charge.

Apart from ^{18}F, only two long-lived emitters could be significantly produced during the irradiation phase, namely ^{11}C ($T_{1/2}$=20.39 minutes) by the reaction ^{10}B(p,γ)^{11}C and ^{13}N ($T_{1/2}$=9.965 minutes) by the reaction ^{12}C(p,γ)^{13}N. The former reaction was found to be negligible from systematic measurements of boron contamination in the targets via the ^{11}B(p,α)2^{4}He reaction (see Fig. 4a). However, a moderate production of ^{13}N had to be taken into account (see below) because of a carbon build-up on the target measured to be about 0.5 μg cm^{-2} per Coulomb of accumulated proton charge. A blank Ta target irradiated in the same experimental conditions showed no β^+ activity but the one due to ^{13}N.

The efficiency ϵ_β for the β^+-activity detection was measured using calibrated ^{22}Na and ^{65}Zn sources. The sources were fixed at the centre of a tantalum foil identical to the ^{17}O target backing and the resulting assembly was positioned between the Ge detectors at the same place as the irradiated targets. With the ^{22}Na source, pulse pile-up due to the emission of the 1.275 MeV γ-ray simultaneously with the two 511 keV ones must be taken into account, especially for high efficiency detection systems. This effect was incorrectly neglected in a previous analysis of our measurement [14] and we detail here how the proper value of ϵ_β already reported in Ref. [15] was obtained. The value obtained without taking into account pile-up effects [14] must be multiplied by the factor

$$r_c = \frac{1}{1 - r(\epsilon_A + \epsilon_B)} \ , \qquad (4)$$

where r=0.904 is the β^+ branching ratio of ^{22}Na [32] and ϵ_A (ϵ_B) the probability for the 1.275 MeV γ-ray to be detected in the detector A (B). ϵ_A and ϵ_B have been measured using the 1.115 MeV line of the ^{65}Zn source which is not affected by pile-up (except accidental pile-up, see below). A correction of 6.5% was applied to the measured ϵ_A and ϵ_B to take into account the difference in energy of the 1.115 and 1.275 MeV lines. Accidental pile-up was minimised by using low-activity sources and short pulse shaping constants. It was finally taken into account as a very small correction (<1%). To account for the finite size of the beam spot on the target during proton irradiation (∼8 mm), the source position was varied by 5 mm from the centre which results in a correcting factor of 0.98±0.02. Many consistent measurements were performed with two different ^{22}Na sources. A number of such efficiency measurements were repeated with a ^{65}Zn source with the advantage of no "true" pile-up effect in that case. The average value from this fully consistent set of measurements was found to be ϵ_β=(4.2 ±0.2)% [15].

The total number of ^{18}F nuclei contained in the targets at the end of the irradiation was measured from a fit of ^{18}F and ^{13}N decay curves to the γ-ray data recorded for ∼6 hours. The best fit was obtained from the maximum of the likelihood function for Poisson-distributed data. The ^{18}F radioactive half-life was set as a free parameter in the fit while the ^{13}N half-life was fixed to $T_{1/2}$=9.965±0.004 minutes [32]. The results are shown in Fig. 7 for irradiation of fresh ^{17}O targets at two energies (on resonance at $E_p^{\rm lab}$=196.5 keV and off resonance at 192.7 keV). The relative contribution of ^{13}N is small at $E_p^{\rm lab}$=196.5 keV, but noticeable off resonance. Also shown in Fig. 7 is the very small background contribution to the 511×511 keV coincident rate which was measured to amount to (1.9±0.2) counts per hour from numerous independent measurements. The total numbers of ^{18}F at the end of the irradiation were 4910±440 at $E_p^{\rm lab}$=196.5 keV (on-resonance) and 422±177 at $E_p^{\rm lab}$=192.7 keV (off-resonance). The value of the ^{18}F half-life from the fit was found to be $T_{1/2}=105^{+19}_{-14}$ minutes (103^{+217}_{-47} minutes) at $E_p^{\rm lab}$=196.5 keV (192.7 keV), which is in excellent (reasonable, inherent to the low statistics) agreement with the actual value of 109.77±0.05 minutes [32]. The experiment was repeated using a fresh ^{17}O target obtained in the same implantation conditions. Fully consistent results were obtained in the two independent measurements.

The far larger number of ^{18}F nuclei produced at the highest beam energy is clearly due to the excitation of the ^{17}O(p,γ)^{18}F resonance at $E_R^{\rm lab}$=194.1 keV. The lower ^{18}F production at $E_p^{\rm lab}$=192.7 keV proceeds from direct capture (DC) interfering with the low-energy part of the resonant capture at $E_R^{\rm lab}$=194.1 keV. The resonance strength was derived after evaluation of the DC cross section (see Sec. III-C-1) and a small contribution of (4.3±2.2)% for DC was subtracted from the ^{18}F total production at $E_p^{\rm lab}$=196.5 keV. We also applied to the measured (p,γ) resonance strength a correction arising from the backscattering of ^{18}F nuclei, which could escape the target at the time of their production. This correction was evaluated to be (4±2)% from calculations performed with the program SRIM-2003 [18] for the estimated implantation profile of the ^{17}O targets.

We finally obtained from the weighted mean of the two measurements at $E_p^{\rm lab}$=196.5 keV: $\omega\gamma_{p\alpha}/\omega\gamma_{p\gamma}$=717±60. The advantage of measuring the strength of the (p,γ) resonance relative to that of the (p,α) channel is that the measured value is free from the uncertainties related to the target composition and the charge measurement. In

the analysis, it was only assumed that the beam intensity was constant during the sub-runs (15 minutes) of the irradiation. The number of emitted α-particles was determined at the end of each sub-run in the same way as described in Sec. II-B-1.

The quoted error in this ratio mainly arises from uncertainties in the measured β^+ activities (statistical uncertainty of 7%), in the associated β^+-detection efficiency (5%), as well as in the measured α-particle intensities (1%) and detection efficiency (3%).

The resulting (p,γ) resonance strength is $\omega\gamma_{p\gamma}=(2.2\pm0.4)\times10^{-6}$ eV, where the uncertainty in the corresponding (p,α) strength is taken into account. Our value is somewhat larger than that obtained in a recent study [9, 11]: $(1.2\pm0.2)\times10^{-6}$ eV. The study of Refs.[9, 11] is different from ours in mainly two basic points: targets prepared by anodization of tantalum in ^{17}O-enriched water, and in-line detection of prompt emitted γ-rays using a large-volume HPGe placed at $\langle\theta\rangle=0^\circ$ very close to the target. The reason for the disagreement between the two measurements is unclear. It cannot be ascribed to the value of the (p,α) resonance strength used as a reference in our study since it appears to be in good agreement with two very recent measurements (see Sec. II-B-2).

The DC cross section has been derived from the measurement at $E_p^{\rm lab}$=192.7 keV according to the equation:

$$Y_{CD} = \int_{\Delta E} \frac{\sigma(E)}{\epsilon(E)} dE \ , \qquad (5)$$

where Y_{CD} is the measured ^{18}F production yield per incident proton, ΔE is the target thickness and $\epsilon(E)$ is the stopping cross section. ΔE and $\epsilon(E)$ were taken from the measured excitation function for the (p,α) resonance. The astrophysical factor $S_{DC}(E)$ was assumed to be constant in the small energy range ΔE. To derive its value, interference between DC and resonant capture at $E_R^{\rm lab}$=194.1 keV was taken into account from a calculation using the present results for the resonance cross section and $S_{DC}(E)$ as estimated in Sec. III-C-1 (see Eq. 13). The corresponding correction amounts to 15%. We finally found S_{DC}=8.3±4.0 keV barn at the effective energy $E_{\rm c.m.}$=180.2 keV, where the large error bar comes essentially from the statistical uncertainty (see Fig. 7).

III. REVISED REACTION RATES FOR THE H-BURNING OF ^{17}O

We have calculated the revised reaction rates for the H-burning of ^{17}O resulting from our experimental results. We have also investigated the DC cross section of the ^{17}O$(p,\gamma)^{18}$F reaction from an analysis of the current data. The general expression for reaction rates is given by (e.g. [10])

$$N_A\langle\sigma v\rangle = N_A \frac{(8/\pi)^{1/2}}{\mu^{1/2}(k_BT)^{3/2}} \int_0^\infty \sigma E \exp(-E/k_BT) dE \ , \qquad (6)$$

where N_A is the Avogadro number, μ the reduced mass of the system, k_B the Boltzmann constant, T the temperature, σ the cross section, v the relative velocity, and E the kinetic energy in the center-of-mass system. We performed numerically the integration of this equation for both resonant and non resonant processes (DC capture). In the Breit-Wigner cross section formula for resonances, we took into account the variation with energy of the partial and total widths of the involved levels, when these quantities are known. It is now the case for the level at 5.7898 MeV in ^{18}F since the partial and total widths of this level can be extracted from the presently measured strengths of the resonances at E_R=183.3 keV (in the following the resonance energies are given in the center-of-mass system, unless mentioned otherwise) in the ^{17}O$(p,\alpha)^{14}$N and ^{17}O$(p,\gamma)^{18}$F reactions and from the previously determined strength of the corresponding resonance at E_R=1.375 MeV in the ^{14}N$(\alpha,\gamma)^{18}$F reaction [12].

For the levels above the reaction threshold, we used the relations:

$$\Gamma_{p,\alpha}(E) \ = \ \Gamma_{p,\alpha}(E_R)\frac{P_l(E)}{P_l(E_R)} \ , \qquad (7)$$

$$\Gamma_\gamma(E) \ = \ \Gamma_\gamma(E_R)\sum_f B_f \left(\frac{E-E_f}{E_R-E_f}\right)^{2\lambda_f+1} \ , \qquad (8)$$

where E_R is the resonance energy, P_l is the penetration factor associated with the relative angular momentum l, B_f is the γ-ray branching ratio to the final state of energy E_f in the compound nucleus and λ_f is the multipolarity of the corresponding γ-ray transition. In the calculation of $\Gamma_\gamma(E)$, we only considered the two decay transitions with the higher branching ratios even when the deexcitation of the involved level is more complex (branching ratios were renormalized in that case). For mixed transitions, we adopted the multipolarity of the dominant transition when the corresponding mixing ratio is known [13], the lowest allowed one otherwise. We checked that for the complex deexcitation level at 5.6716 MeV the inferred difference in reaction rate values compared to exact calculation is lower than 0.25%. In the calculation of P_l, the channel radius was obtained with r_0=1.25 fm.

For the sub-threshold levels, the proton partial width is given by

$$\Gamma_p(E) = 2P_l(E)C^2S\theta_{sp}^2 \ , \qquad (9)$$

with C^2S being the spectroscopic factor and θ_{sp}^2 the single-particle reduced width.

The so-called level shift [33] was also introduced in the Breit-Wigner expression when necessary (i.e. when the proton width amounts to more than 10% of its maximum value).

A. Widths of the level at 5.7898 MeV in ^{18}F

From the values $\omega\gamma_{p\gamma}$=(2.2±0.4)×10^{-6} eV and $\omega\gamma_{p\alpha}$=(1.6±0.2)×10^{-3} eV measured in this study for the strengths of the E_R=183.3 keV resonances, and from $\omega\gamma_{\alpha\gamma}$=(1.57±0.60)×10^{-2} eV taken from Ref. [12] for the resonance at E_R=1375 keV in the reaction ^{14}N(α,γ)^{18}F, the values of the proton, α, γ and total widths of the level at 5.7898 MeV in ^{18}F are found to be Γ_p=(0.38±0.05)×10^{-2} eV, Γ_α=6.8±3.0 eV, Γ_γ=(0.94±0.36)×10^{-2} eV and Γ=6.8±3.0 eV, respectively. With these values, the total width is found consistent with the measured level lifetime: $\tau\leq$2.6 fs. It is in disagreement with the previous value of (15±10) fs given in Ref. [12]. The large error bars on Γ_α, Γ_γ and Γ come essentially from the uncertainty in $\omega\gamma_{\alpha\gamma}$ [12].

B. The ^{17}O(p,α)^{14}N reaction rate

In the calculation of the ^{17}O(p,α)^{14}N reaction rate, we considered the levels in ^{18}F at 5.6034, 5.6716 and 5.7898 MeV and fifteen levels at higher energies as done in Ref. [10]. Revised values were obtained for the rate contributions of the three lowest levels. An interference effect between the presently observed resonance at E_R=183.3 keV and that at E_R=1202.5 keV was also investigated. Contributions from the other levels are the same as in Ref. [10] (see page 91 of Ref. [10] for the adopted resonance strengths). The parameters of the six most important levels in ^{18}F for the total rate at T<0.3 GK are summarized in Table I.

The proton width of the sub-threshold level at 5.6034 MeV was revaluated by calculating its single-particle reduced width using a Woods-Saxon potential with the same parameters that were adopted in Ref. [36] to extract the spectroscopic factor. The resulting proton width is lowered by a factor of ∼3 compared to Refs. [10, 36] where the single-particle reduced width was identified with the Wigner limit. For this sub-threshold state, the level shift was introduced in the Breit-Wigner formula with a mean effect of ∼5% on the calculated rates.

The total reaction rates are given by an incoherent sum of the individual contributions of the involved resonances. The only exception is for the resonance at E_R=183.3 keV whose interference with the broad one at E_R=1202.5 keV (Γ=79±5 keV [35]) was considered using the two-level approximation given in Ref. [37]. The effect was found to be weak and was introduced as a small increase in the uncertainty in the rate for temperatures between 0.1 and 0.2 GK.

The calculated total reaction rates are given in Table II for temperatures of T=0.01–1.5 GK, together with lower and upper limits corresponding to 1σ confidence level. If the modal rate was calculated by numerical integration as already indicated, the uncertainties corresponding to the given limits were obtained from propagation of the statistical errors on the involved parameters using the well-known approximate relations [10]:

$$N_A\langle\sigma v\rangle_R = 1.5394\times10^{11}(AT_9)^{-3/2}(\omega\gamma)\times \exp(-11.605E_R/T_9)\ , \quad (10)$$

$$N_A\langle\sigma v\rangle_{\rm tail} = 7.8318\times10^{9}(Z_pZ_t/A)^{1/3}S(E_0)T_9^{-2/3}\times \exp(-4.2486(Z_p^2Z_t^2A/T_9)^{1/3})\ , \quad (11)$$

where $N_A\langle\sigma v\rangle_R$ gives the resonant contribution of a given resonance and $N_A\langle\sigma v\rangle_{\rm tail}$ represents the "tail contribution" of the considered resonance. Here the rates are expressed in cm^3 mol^{-1} s^{-1}, the center of mass energy E_R and the resonance strength $\omega\gamma$ are given in MeV, T_9 is the temperature in units of GK, A is the reduced mass in amu, and $S(E_0)$ is the astrophysical factor at the so-called Gamow energy:

$$E_0\ ({\rm MeV}) = 0.1220(Z_p^2Z_t^2AT_9^2)^{1/3}\ , \quad (12)$$

with Z_p and Z_t being the projectile and target atomic numbers, respectively. In computing error propagation, we used the formalism given in Ref. [38]. The contributions to $N_A\langle\sigma v\rangle$ of the resonance tails were found to be small for T_9>0.03. But at lower temperatures, the tail contributions from the subthreshold level at E_x=5.6034 MeV and from the level at E_x=5.6716 MeV are dominant (see Fig. 8) and the associated errors were computed by error propagation through Eq. (11). We calculated the error in $S(E_0)$ taking into account both uncertainties in resonance energy and strength, as it is done in Ref. [38] for the resonant contribution (Eq. 10). The uncertainty in a weak component of the rate (∼10%, see Fig. 8) due to the relatively broad resonance at E_R=1202.5 keV was also taken into account in the same way.

To check the reliability of the so-calculated errors, we performed a full Monte Carlo simulation at a few given temperatures. Random values for the involved parameters of the levels at 5.603 and 5.672 MeV (partial and total widths, level energies as well as Q values for ^{17}O+p→^{18}F and ^{14}N+α→^{18}F) were generated according to the corresponding errors (see Table 1 and Ref. [26]). They were assumed to have a Gaussian distribution. The limits for $N_A\langle\sigma v\rangle$ were obtained from calculation of the probability density of $N_A\langle\sigma v\rangle$ after numerical integration. The errors calculated from this "exact" but time-consuming procedure were found to be very similar to those obtained from the above-described analytical procedure. The same check was performed for a few temperatures above T_9=0.04 on the narrow resonant level at 5.7898 MeV. We also obtained a very good agreement. Finally, the limits given in Table II are the results of the analytical calculations in the whole temperature range.

Ratios of individual reaction rate contributions and the total modal rate are displayed in Fig. 8 as a function of temperature. The strong effect of the previously unknown resonance at E_R=183.3 keV is clearly visible since this resonance dominates the total reaction rates

in the temperature range (1–4)×10^8 K which is of most importance in nova nucleosynthesis. Below T_9=0.02, the dominant contributions arise from the levels at 5.603 and 5.672 MeV with a small component due to the broad high-energy levels at 6.163, 6.633 and 6.809 MeV.

We show in Fig. 9 a comparison of present and previous [10] total reaction rates for the ^{17}O(p,α)^{14}N reaction. Also given are the associated uncertainties. Large differences can be seen in both ranges T_9<0.02 and T_9=0.1–0.4. For T_9<0.02, the difference is mainly to be ascribed to the lowered value of the single particle width of the subthreshold level at 5.603 MeV. In the temperature range of T_9=0.1–0.4, the reaction rate increase of more than an order of magnitude is due to the present observation of the previously unknown resonance at E_R=183.3 keV. The slight difference observed between T_9=0.02 and T_9=0.1 (∼30%) originates in the revaluation of the excitation energy of the level at 5.6716 MeV.

Besides the very large differences with previous studies found in the range of temperatures attained during nova outbursts, the second important point shown in Fig. 9 is the drastic improvement in accuracy observed for T_9=0.1–0.4. For example, at T_9=0.2, the uncertainty in the reaction rate is reduced from more than two orders of magnitude to ∼15% due to the precise measurement of the strength of the resonance at E_R=183.3 keV, whereas estimating the latter strength previously was some tricky guessing game. The two very recent measurements of the strength of this resonance at Oak Ridge National Laboratory [30] and Triangle Universities Nuclear Laboratory [31] will probably allow to further reduce the uncertainty of the ^{17}O(p,α)^{14}N reaction rate in the range T_9=0.1–0.4, as it appears that the results obtained in these experiments are fully compatible with those from the present work.

C. The ^{17}O(p,γ)^{18}F reaction rate

In the calculation of the ^{17}O(p,γ)^{18}F rate, we considered the levels at 5.6033, 5.6716 and 5.7898 MeV in the same way as for the ^{17}O(p,α)^{14}N reaction (see Table I for the adopted level parameters) and sixteen levels above E_R=183.3 keV. For the latter contributions, we followed the study of Ref. [10] (see page 89 of that reference for the resonance strength values) except for the resonance at E_R=489.9 keV for which we used a new measurement [11] of the resonance strength and for the resonance at E_R=501.5 keV for which the wrong limit ($\omega\gamma_{p\gamma}$<0.33) quoted in Ref. [10] was corrected to the value of $\omega\gamma_{p\gamma}$<0.33×10^{-3} given in Ref [12].

As already pointed out [10, 11, 39], the direct capture process strongly affects the total reaction rates for T_9<0.8. In Refs. [10, 36, 39], the DC contribution was extrapolated from high-energy experimental cross sections of Ref. [39]. Recently, Fox *et al.* [11] employed an alternative method based on theoretical calculations. A Woods-Saxon single-particle potential served to generate the radial wave functions of the 21 final bound states in ^{18}F to which E1 DC transitions are allowed. The spectroscopic factors of the 21 considered levels were taken from the literature. The total $S_{DC}(E)$ values were finally obtained as an incoherent sum of the calculated individual contributions. We have re-examined the evaluation of the cross sections for the DC process in the ^{17}O(p,γ)^{18}F reaction in view of its strong influence on the total reaction rate.

1. *Analysis of the direct capture contribution*

We show in Fig. 10 the existing experimental measurements of the DC cross sections in ^{17}O(p,γ)^{18}F (Ref. [39] and the present low-energy measurement described in Sec. II-C-2). In his study [39], Rolfs assumed a pure DC process in the energy ranges $E_{\rm c.m.}$=0.27–0.44 MeV and $E_{\rm c.m.}$=0.88–1.78 MeV (see Fig. 11 of Ref. [39]). On the contrary, Fox *et al.* [11] argue that the data points in the low-energy range should be "influenced by the tails of higher lying broad resonances", as indicated by their calculation of the incoherent sum of the cross sections from the broad resonances at E_R=556.7 keV and E_R=676.7 keV. Then, as the energy dependence obtained in Ref. [39] using a square-well potential is quite different from the one they calculate using more realistic Woods-Saxon potentials, they conclude that "it is surprising that the extrapolated S-factor of Ref. [39] agrees with the four low-energy data points" given in the same study in the energy range $E_{\rm c.m.}$=0.27–0.44 MeV. In view of this argument, they finally disregard all the data points of Ref. [39] (including those above $E_{\rm c.m.}$=0.88 MeV) and rely on calculations based on measured spectroscopic factors to estimate the absolute scale of the DC cross section. The calculations are described in detail in Ref. [11] and the obtained results are displayed in Fig. 10. The disagreement with the experimental values (Ref. [39] and this work) is evident for the low- and high-energy data points.

We reinvestigated the DC process S-factor by correcting the low-energy data points of Ref. [39] from the contribution of the broad resonances at E_R=556.7 keV and E_R=676.7 keV according to the statement of Ref. [11]. The corrections were calculated from the Breit-Wigner formula with energy-dependent partial widths (see Table I for the values at the resonance energies). The DC cross sections were then calculated in the same way that was used in Ref. [11] (i.e. with a Woods-Saxon potential) except for the used specific computer code (code RACAP obtained from P. Descouvement, private communication). We obtained very similar results for the shape of the S-factor energy dependence and for its magnitude as well. In an attempt to fit the quadratic function describing the so-calculated energy dependence to the whole set of data, we simulated the high-energy (>0.88 MeV) results of Ref. [39] by a set of 19 points distributed according to the spread of the corresponding data as appreciated from Fig. 17 of Ref. [39] (see Fig. 10).

The result of the fit is given as a solid line in Fig. 10. It is clear from this figure that the energy dependence calculated with a Woods-Saxon potential is inconsistent with the high-energy data points of Ref. [39], given their very small estimated relative error bars (∼3%). With this fit, we get for the DC S-factor:

$$S_{DC}(E) = 6.2 + 1.61E - 0.169E^2 \qquad (13)$$

where E is in MeV and $S_{DC}(E)$ in keV barn.

This result is not significantly dependent on the way we simulated the high-energy results of Ref. [39] (e.g. the number of representative data points). If the fit is restricted to the five low-energy points for lack of a detailed report of the high-energy results in Ref. [39], the obtained $S_{DC}(E)$ is 13% higher.

In an attempt to understand the inconsistency of the data above 0.88 MeV with the $S_{DC}(E)$ of Eq. (13), we corrected the simulated high-energy data points from the contributions of the broad resonances at 556.7, 676.7 and 1170 keV. These contributions, calculated from the resonance parameters given in table I and in Ref. [13], were found to be non negligible (15% at the maximum) in a significant part of the high-energy range of the data of Ref. [39]. Fitting a quadratic function proportional to that of Eq. (13) to the so-corrected data and assuming relative error bars of 5% for these data, we obtained a fit of good quality ($\chi^2_{\rm red}$=1.3). The corresponding $S_{DC}(E)$ values are lowered by 3% compared to those given by Eq. (13). This result suggests that many of the data points of Ref. [39], in both the low- and high-energy ranges, could suffer from some mixing of DC and resonant processes. Obviously, new data which could allow to clearly disentangle the DC cross section from resonance contributions would be highly valuable. However, we retained in the present work the relation (13) as the final result for $S_{DC}(E)$. But considering the bad quality of the corresponding fit and following a suggestion of Ref. [11], we took the overall fractional uncertainty in $S_{DC}(E)$ to be 50%.

The present $S_{DC}(E)$ values are higher by a factor of ∼1.7 than those given in Ref. [11], but still in agreement with them given the uncertainty of 50% estimated in both studies. At low energy, they are lower than those given in Ref. [39] (see Fig. 10), essentially due to the Woods-Saxon potential used in the present work in place of the square-well potential of Ref. [39].

The DC contribution to the total rate was calculated by numerical integration of Eq. (6). Interference between DC and resonant capture was neglected since these processes mainly proceed through different orbital angular momenta and/or different γ-ray multipolarities. Note that the interference effect considered in the analysis of the present (p,γ) measurement at $E_p^{\rm lab}$=192.7 keV (Sec.II-C-2) only affects the S-factor value near $E_{\rm c.m.}$=180 keV. It was checked that its effect on the reaction rate is negligible.

2. Total reaction rates

Total reaction rates and lower and upper limits corresponding to 1σ confidence level were calculated using the procedure described above for the ^{17}O$(p,\alpha)^{14}$N reaction. The results are listed in Table III for temperatures of T_9=0.01–1.5. The main uncertainty in the ^{17}O$(p,\gamma)^{18}$F rate comes from the DC contribution (50%). Clearly, additional measurements of the DC cross sections of the ^{17}O$(p,\gamma)^{18}$F reaction including more precise studies at low energy (E<0.4 MeV) would be highly valuable to further reduce this uncertainty.

Individual rate contributions relative to the total modal rate are shown in Fig. 11. The direct capture process dominates the total rate below T_9=0.03 and in the range T_9=0.09–0.4. This indicates that the importance of the resonance at $E_{\rm c.m.}$=183.3 keV is less pronounced than in the ^{17}O$(p,\alpha)^{14}$N case, but its contribution is still significant around T_9=0.2.

Ratios of present to previous [10, 11] total reaction rates for ^{17}O$(p,\gamma)^{18}$F are shown in Fig. 12. The modal rates are given as well as the lower and upper limits. The comparison with the NACRE compilation [10] shows (see Fig. 12a) that the modal rates are in agreement above T_9=0.4, whereas the present upper limit is significantly lower due to the corrected value used for the strength of the resonance at E_R=501.5 keV. Between T_9=0.1 and T_9=0.4, the present rates are smaller than the NACRE values by up to a factor ∼5, but still within the previous very large error bars mainly caused by the unmeasured resonance at 183.3 keV. It can be seen from Fig. 12a that the fractional uncertainty in the rates (about ±30% in the present study) has been reduced by more than two orders of magnitude in this temperature range. Below T_9=0.1, a smaller reduction of the rate values is observed, which is mainly due to our analysis of the DC contribution.

The comparison with the recent work of Ref. [11] shown in Fig. 12b indicates moderate differences which are to be ascribed to a different estimation of the DC cross section and to the somewhat divergent values obtained for the strength of the resonance at 183.3 keV.

IV. SUMMARY AND CONCLUSIONS

We reported on the observation of a previously undiscovered resonance at $E_{\rm c.m.}$=183.3±0.6 keV in the ^{17}O$(p,\alpha)^{14}$N reaction, with a measured resonance strength $\omega\gamma_{p\alpha}$=(1.6±0.2)×10^{-3} eV. The strength of the ^{17}O$(p,\gamma)^{18}$F resonance at the same energy was measured to be $\omega\gamma_{p\gamma}$=(2.2±0.4)×10^{-6} eV by an activation method. From these values combined with the known strength of the ^{14}N$(\alpha,\gamma)^{18}$F resonance feeding the same level, we calculated the partial and total widths of the ^{18}F level at E_x=5.7898 MeV. The lifetime of this level was also measured by DSAM and the observed limit was found to be consistent with the total width calculated from partial widths, contrary to a previous DSAM measurement [12].

A precise value of the excitation energy of the resonant level was also obtained in the lifetime measurement.

We calculated the ^{17}O+p thermonuclear rates using the presently measured properties of the ^{18}F level at E_x=5.7898 MeV and clarifying the situation for the subthreshold state at 5.6034 MeV and for the level at 5.6716 MeV. In the analysis of the ^{17}O(p,γ)^{18}F rate, the contribution of the DC process was revisited, with the conclusion that new data would be helpful to further reduce the potential systematic uncertainties in this reaction rate. The previous uncertainties in the ^{17}O+p rates are finally reduced by orders of magnitude at temperatures in the range 0.1–0.4 GK. The rate uncertainties are now reasonably small, especially for the ^{17}O(p,α)^{14}N rate, which can be considered to be firmly established below 1.5 GK.

As shown in Ref. [14] from hydrodynamic simulations of classical nova outbursts, the results of the experiments described in this paper have important consequences for ^{17}O and ^{18}F nucleosynthesis in classical novae. Besides the ^{17}O+p rates, the final abundance of ^{18}F in nova ejecta is also strongly dependent on the rate of the reaction ^{18}F(p,α)^{15}O, which is presently the subject of strong experimental efforts (e.g. [40–42]). A significant reduction of the uncertainty in this reaction rate should soon allow accurate predictions for the synthesis of ^{17}O and ^{18}F in nova outbursts.

Acknowledgments

We wish to thank E. Virassamynaiken and D. Ledu for the preparation of the TiN and O-implanted targets, respectively, as well as the technical staff of the CSNSM for their constant help. We are also indebted to C. Iliadis for several useful discussions. This work was supported by the CMEP agreement for scientific cooperation between France and Algeria under the project No. 01MDU518 and by AYA2004-06290-C02.

[1] M. J. Harris, D. L. Lambert, and V. V. Smith, Astrophys. J. **325**, 768 (1988).
[2] L. R. Nittler, C. M. O'D Alexander, X. Gao, R. M. Walker, and E. K. Zinner, Nature **370**, 443 (1994).
[3] L. R. Nittler and R. Cowsik, Phys. Rev. Lett. **78**, 175 (1997).
[4] A. I. Boothroyd, I.-J. Sackmann, and G. J. Wasserburg, Astrophys. J. **430**, L77 (1994).
[5] J. José and M. Hernanz, Astrophys. J. **494**, 680 (1998).
[6] S. Starrfield, J. W. Truran, M. Wiescher, and W. M. Sparks, Mon. Not. R. Astron. Soc. **296**, 502 (1998).
[7] J. Gómez-Gomar, M. Hernanz, J. José, and J. Isern, Mon. Not. R. Astron. Soc. **296**, 913 (1998).
[8] A. Coc, M. Hernanz, J. José, and J.-P. Thibaud, Astron. Astrophys. 357, 561 (2000).
[9] C. Fox, C. Iliadis, A. E. Champagne, A. Coc, J. José, R. Longland, J. Newton, J. Pollanen, and R. Runkle, Phys. Rev. Lett. **93**, 081102 (2004).
[10] C. Angulo *et al.*, Nucl. Phys. **A656**, 3 (1999).
[11] C. Fox, C. Iliadis, A. E. Champagne, R. P. Fitzgerald, R. Longland, J. Newton, J. Pollanen, and R. Runkle, Phys. Rev. C **71**, 055801 (2005).
[12] C. Rolfs, I. Berka, and R. E. Azuma, Nucl. Phys. **A199**, 306 (1973).
[13] D. R. Tilley, H. R. Weller, C. M. Cheves, and R. M. Chasteler, Nucl. Phys. **A595**, 1 (1995).
[14] A. Chafa *et al.*, Phys. Rev. Lett. **95**, 031101 (2005).
[15] A. Chafa *et al.*, Phys. Rev. Lett. **96**, 019902(E) (2006).
[16] P. J. Nolan, F. A. Beck, and D. B. Fossan, Annu. Rev. Nucl. Part. Sci. **44**, 561 (1994).
[17] D.C. Radford, Nucl. Instr. Meth. **A361**,297 (1995).
[18] J. F. Ziegler and J. P. Biersack, Program SRIM-2003 (unpublished). See also URL http://www.srim.org/
[19] A. E. Blaugrund, Nucl. Phys. **88**, 501 (1966).
[20] I. Berka, K. P. Jackson, C. Rolfs, A. M. Charlesworth, and R. E. Azuma, Nucl. Phys. **A288**, 317 (1977).
[21] CERN Program Library Office (Online), Available at: http://www.info.cern.ch/asdoc/geant_html3/geantall.html.
[22] T. K. Alexander and J.S. Forster, Advances in Nucl. Phys. 10, 197 (1968).
[23] H.-B. Mak, G. T. Ewan, H. C. Evans, J. D. MacArthur, W. McLatchie, and R. E. Azuma, Nucl. Phys. **A343**, 79 (1980).
[24] G. Bogaert, V. Landré, P. Aguer, S. Barhoumi, M. Kious, A. Lefebvre, J. P. Thibaud, and D. Bertault, Phys. Rev. C **39**, 265 (1989).
[25] F. Ajzenberg-Selove, Nucl. Phys. **A523**, 1 (1991).
[26] G. Audi, A. H. Wapstra, and C. Thibault, Nucl. Phys. **A729**, 337 (2003).
[27] G. Bogaert *et al.*, Nucl. Instr. Meth. **B89**, 8 (1994).
[28] H. W. Becker *et al.*, Z. Phys. **A351**, 453 (1995).
[29] H. Lorenz-Wirzba, P. Schmalbrock, H. P. Trautvetter, M. Wiescher, C. Rolfs, and W. S. Rodney, Nucl. Phys. **A313**, 346 (1979).
[30] B. H. Moazen et al., submitted to Phys. Rev. C. The quoted results are $\omega\gamma_{p\alpha}$=(1.70±0.15)×10^{-3} eV and $E_{\rm c.m.}$=183.5$^{+0.1}_{-0.4}$ keV for the resonance strength and energy, respectively.
[31] C. Iliadis, private communication.
[32] NuDaT database, http://www.nndc.bnl.gov/nudat2/.
[33] R. G. Thomas, Phys. Rev. **81**, 148 (1951).
[34] H. W. Becker, W. E. Kieser, C. Rolfs, H. P. Trautvetter, and M. Wiescher, Z. Phys. **A305**, 319 (1982).
[35] R. E. Brown, Phys. Rev. **125**, 347 (1962).
[36] V. Landré, P. Aguer, G. Bogaert, A. Lefebvre, J.-P. Thibaud, S. Fortier, J.-M. Maison, and J. Vernotte, Phys. Rev. C **40**,1972 (1989).
[37] C. Rolfs and W. S. Rodney, Nucl. Phys. **A250**, 295 (1975).
[38] W.J. Thomson and C. Iliadis, Nucl. Phys. **A647**, 259 (1999).
[39] C. Rolfs, Nucl. Phys. **A217**, 29 (1973).
[40] N. de Séréville *et al.*, Phys. Rev. C **67**, 052801(R) (2003).
[41] R. L. Kozub *et al.*, Phys. Rev. C **71**, 032801 (2005).

[42] N. de Séréville *et al.*, Nucl. Phys. **A** (in press).

TABLE I: Summary of the parameters of the six most important levels in ^{18}F for the ^{17}O(p,α)^{14}N and ^{17}O(p,γ)^{18}F reaction rates at temperatures T<0.3 GK.

E_R[a] (keV)	E_x (keV)	J^π	Γ_p (eV)	Γ_α (eV)	Γ_γ (eV)
-3.12±0.57	5603.38±0.27[b]	1^+	–[c]	42.8±1.6[d]	0.485±0.046[d]
65.1±0.5	5671.6±0.2[e]	1^-	$(19\pm3)\times10^{-9}$[f]	130±5[d]	0.45±0.02[g]
183.3±0.6	5789.8±0.3[e]	2^-	$(3.8\pm0.5)\times10^{-3}$[e]	6.8±3.0[e]	$(9.4\pm3.6)\times10^{-3}$[e]
556.7±1.0	6163.2±0.9[b]	3^+	$(14.0\pm0.5)\times10^{3}$[h]	3.86±0.72[h]	$(37.7\pm8.6)\times10^{-2}$[h]
676.7±1.0	6283.2±0.9[b]	2^+	$(10.0\pm0.5)\times10^{3}$[h]	13.9±0.5[h]	0.64±0.14[h]
1202.5±5.0	6809±5[b]	2^-	14.5×10^{3}[i]	64.5×10^{3}[i]	–

[a]Based on the Q-value for ^{17}O+$p\rightarrow^{18}$F: Q=5606.5±0.5 keV [26].
[b]From Ref. [13].
[c]$\Gamma_p(E)$ calculated from Eq. (9) with C^2S=0.12±0.04 [36] and θ^2_{sp}=0.89 MeV (this work).
[d]From Ref. [23].
[e]From present work (see text).
[f]From Ref. [11].
[g]From Ref. [34].
[h]Based on the resonance strengths $\omega\gamma_{p\gamma}$ and $\omega\gamma_{p\alpha}$ from Ref. [10] and the total width Γ from Ref. [13].
[i]From Ref. [35], which also gives $\omega\gamma_{p\alpha}=(4.93\pm0.34)\times10^3$ eV and $\Gamma=(79\pm5)\times10^3$ eV. We did not take into account other values of Γ given in the literature, because they could include extra contributions from higher-energy levels (see [35]). The partial width Γ_γ of this level is not known.

TABLE II: Total thermonuclear reaction rates for $^{17}O(p,\alpha)^{14}N$.

T (GK)	Lower limit	Modal rate	Upper limit
0.01	4.02×10^{-25}	4.97×10^{-25}	5.92×10^{-25}
0.011	4.27×10^{-24}	5.23×10^{-24}	6.18×10^{-24}
0.012	3.50×10^{-23}	4.24×10^{-23}	4.99×10^{-23}
0.013	2.31×10^{-22}	2.79×10^{-22}	3.26×10^{-22}
0.014	1.29×10^{-21}	1.54×10^{-21}	1.80×10^{-21}
0.015	6.23×10^{-21}	7.44×10^{-21}	8.65×10^{-21}
0.016	2.75×10^{-20}	3.26×10^{-20}	3.77×10^{-20}
0.018	5.12×10^{-19}	6.19×10^{-19}	7.26×10^{-19}
0.02	1.11×10^{-17}	1.53×10^{-17}	1.94×10^{-17}
0.025	1.10×10^{-14}	1.54×10^{-14}	1.99×10^{-14}
0.03	1.30×10^{-12}	1.76×10^{-12}	2.22×10^{-12}
0.04	4.77×10^{-10}	6.14×10^{-10}	7.52×10^{-10}
0.05	1.52×10^{-8}	1.92×10^{-8}	2.32×10^{-8}
0.06	1.46×10^{-7}	1.81×10^{-7}	2.17×10^{-7}
0.07	7.09×10^{-7}	8.73×10^{-7}	1.04×10^{-6}
0.08	2.28×10^{-6}	2.79×10^{-6}	3.30×10^{-6}
0.09	5.96×10^{-6}	7.16×10^{-6}	8.36×10^{-6}
0.1	1.56×10^{-5}	1.80×10^{-5}	2.05×10^{-5}
0.11	4.62×10^{-5}	5.20×10^{-5}	5.77×10^{-5}
0.12	1.45×10^{-4}	1.64×10^{-4}	1.83×10^{-4}
0.13	4.35×10^{-4}	4.96×10^{-4}	5.57×10^{-4}
0.14	1.18×10^{-3}	1.35×10^{-3}	1.52×10^{-3}
0.15	2.85×10^{-3}	3.27×10^{-3}	3.69×10^{-3}
0.16	6.19×10^{-3}	7.12×10^{-3}	8.04×10^{-3}
0.18	2.25×10^{-2}	2.59×10^{-2}	2.92×10^{-2}
0.2	6.25×10^{-2}	7.18×10^{-2}	8.11×10^{-2}
0.25	3.84×10^{-1}	4.39×10^{-1}	4.94×10^{-1}
0.3	1.48×10^{0}	1.65×10^{0}	1.82×10^{0}
0.35	6.02×10^{0}	6.50×10^{0}	6.97×10^{0}
0.4	2.56×10^{1}	2.75×10^{1}	2.94×10^{1}
0.45	9.28×10^{1}	9.99×10^{1}	1.07×10^{2}
0.5	2.73×10^{2}	2.95×10^{2}	3.16×10^{2}
0.6	1.42×10^{3}	1.53×10^{3}	1.63×10^{3}
0.7	4.64×10^{3}	4.96×10^{3}	5.28×10^{3}
0.8	1.12×10^{4}	1.20×10^{4}	1.27×10^{4}
0.9	2.24×10^{4}	2.38×10^{4}	2.51×10^{4}
1.	3.91×10^{4}	4.12×10^{4}	4.34×10^{4}
1.25	1.09×10^{5}	1.14×10^{5}	1.19×10^{5}
1.5	2.29×10^{5}	2.38×10^{5}	2.47×10^{5}

TABLE III: Total thermonuclear reaction rates for $^{17}O(p,\gamma)^{18}F$.

T (GK)	Lower limit	Modal rate	Upper limit
0.01	2.37×10^{-25}	4.55×10^{-25}	6.73×10^{-25}
0.011	2.52×10^{-24}	4.84×10^{-24}	7.15×10^{-24}
0.012	2.04×10^{-23}	3.91×10^{-23}	5.79×10^{-23}
0.013	1.32×10^{-22}	2.54×10^{-22}	3.76×10^{-22}
0.014	7.14×10^{-22}	1.37×10^{-21}	2.03×10^{-21}
0.015	3.30×10^{-21}	6.34×10^{-21}	9.37×10^{-21}
0.016	1.34×10^{-20}	2.57×10^{-20}	3.80×10^{-20}
0.018	1.60×10^{-19}	3.07×10^{-19}	4.53×10^{-19}
0.02	1.39×10^{-18}	2.62×10^{-18}	3.85×10^{-18}
0.025	1.47×10^{-16}	2.37×10^{-16}	3.26×10^{-16}
0.03	8.02×10^{-15}	1.08×10^{-14}	1.36×10^{-14}
0.04	2.10×10^{-12}	2.66×10^{-12}	3.23×10^{-12}
0.05	6.55×10^{-11}	8.19×10^{-11}	9.83×10^{-11}
0.06	6.66×10^{-10}	8.27×10^{-10}	9.89×10^{-10}
0.07	3.60×10^{-9}	4.55×10^{-9}	5.50×10^{-9}
0.08	1.35×10^{-8}	1.78×10^{-8}	2.22×10^{-8}
0.09	4.09×10^{-8}	5.77×10^{-8}	7.44×10^{-8}
0.1	1.12×10^{-7}	1.68×10^{-7}	2.23×10^{-7}
0.11	2.95×10^{-7}	4.54×10^{-7}	6.13×10^{-7}
0.12	7.53×10^{-7}	1.16×10^{-6}	1.57×10^{-6}
0.13	1.84×10^{-6}	2.79×10^{-6}	3.74×10^{-6}
0.14	4.25×10^{-6}	6.29×10^{-6}	8.33×10^{-6}
0.15	9.16×10^{-6}	1.32×10^{-5}	1.73×10^{-5}
0.16	1.84×10^{-5}	2.61×10^{-5}	3.38×10^{-5}
0.18	6.13×10^{-5}	8.50×10^{-5}	1.09×10^{-4}
0.2	1.66×10^{-4}	2.27×10^{-4}	2.89×10^{-4}
0.25	1.07×10^{-3}	1.48×10^{-3}	1.89×10^{-3}
0.3	4.24×10^{-3}	5.98×10^{-3}	7.71×10^{-3}
0.35	1.53×10^{-2}	2.08×10^{-2}	2.62×10^{-2}
0.4	5.73×10^{-2}	7.20×10^{-2}	8.67×10^{-2}
0.45	2.01×10^{-1}	2.38×10^{-1}	2.75×10^{-1}
0.5	6.02×10^{-1}	6.95×10^{-1}	7.89×10^{-1}
0.6	3.41×10^{0}	3.88×10^{0}	4.35×10^{0}
0.7	1.21×10^{1}	1.37×10^{1}	1.53×10^{1}
0.8	3.14×10^{1}	3.55×10^{1}	3.95×10^{1}
0.9	6.57×10^{1}	7.38×10^{1}	8.19×10^{1}
1.	1.18×10^{2}	1.32×10^{2}	1.45×10^{2}
1.25	3.26×10^{2}	3.64×10^{2}	4.03×10^{2}
1.5	6.34×10^{2}	6.98×10^{2}	7.62×10^{2}

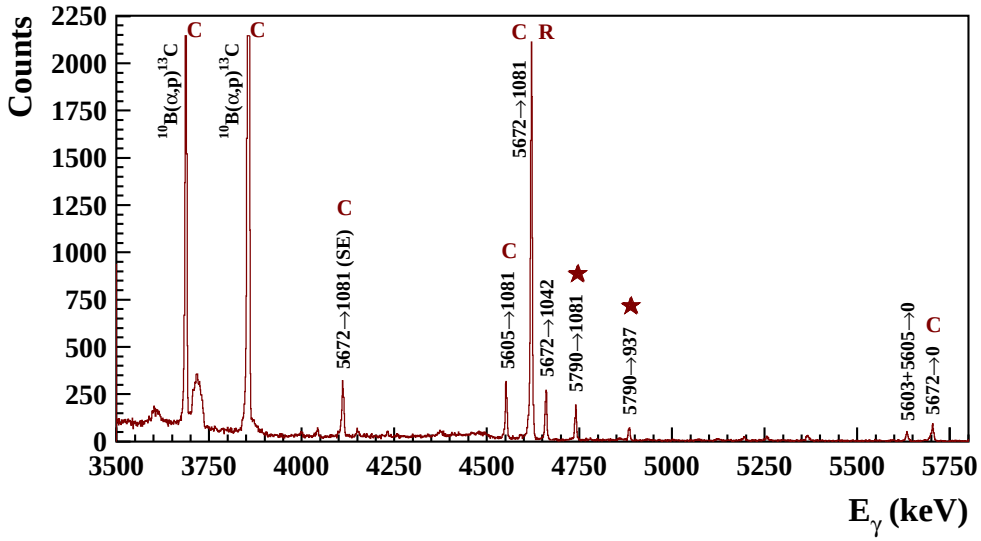

FIG. 1: (Color online) Section of a typical γ-ray spectrum obtained at $E_\alpha^{\rm lab}$=1775 keV with the HPGe detector at $\theta_{\rm lab}$=0°. The two resonances corresponding to the 5671.6 and 5789.8 keV levels in ^{18}F were simultaneously populated. A small component due to the weak excitation of the resonant levels at 5603–5605 keV is also visible. The ordinate scale of the figure has been chosen to illustrate some γ-ray peaks of relatively low intensities, leading to a truncated drawing for the two lines arising from the ^{10}B(α,p)^{13}C reaction. The labels "C" and "R" indicate some of the lines used for calibration and the reference peak for energy difference measurements, respectively (see text). The primary γ-ray decays of the resonant level at 5790 keV are labeled with stars. All lines correspond to full-energy peaks unless labeled SE (single-escape line).

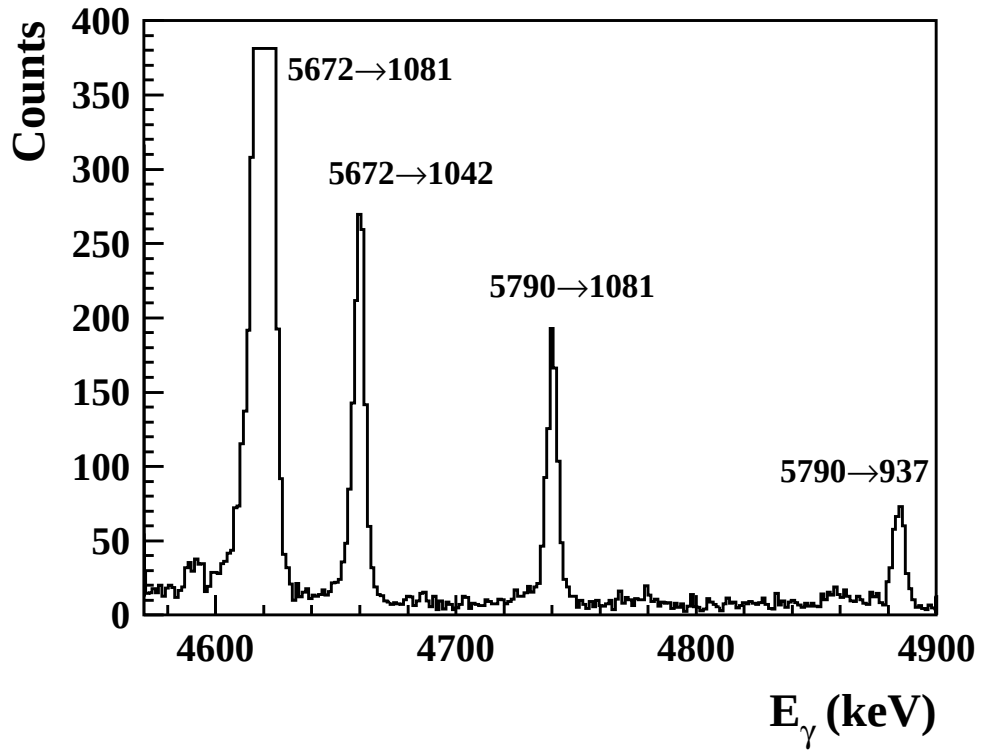

FIG. 2: Relevant section of the γ-ray spectrum shown in Fig. 1, taken at $\theta_{\rm lab}$=0° for $E_\alpha^{\rm lab}$=1775 keV. The ordinate scale of the figure has been chosen to illustrate the primary γ-ray decays of the resonant level at 5790 keV leading to a truncated drawing for the 5672→1081 keV reference line. The observed weak peak below the 5672→1081 keV line, identified to the full Doppler-shifted 5603+5605→0 keV double-escape line, has been included in the least-square fits for energy measurements.

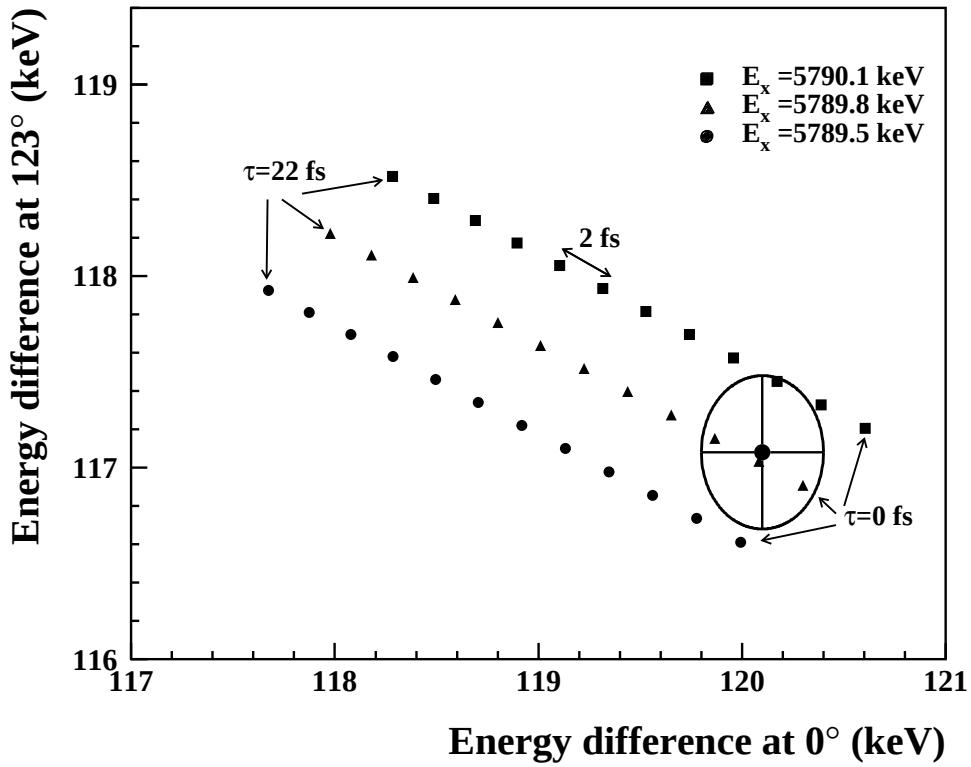

FIG. 3: Calculated and measured values of the differences Δ_i in the energy of the transitions 5790→1081 keV and 5671.6→1081 keV plotted in the plane Δ_0–Δ_1 (the subscript 0(1) refers to values obtained at 0°(123°)). Δ_i is calculated for lifetimes of the level at 5790 keV in the range 0–22 fs by a step of 2 fs. The calculated values are given for three different excitation energy values for the level at 5790 keV. As indicated in the text, the lifetime of the 5671.6 keV level is short enough to induce full Doppler shifts of the associated lines. The experimental value is given together with the covariance ellipse corresponding to the bivariate normal distribution of the two independent random variables Δ_0 and Δ_1.

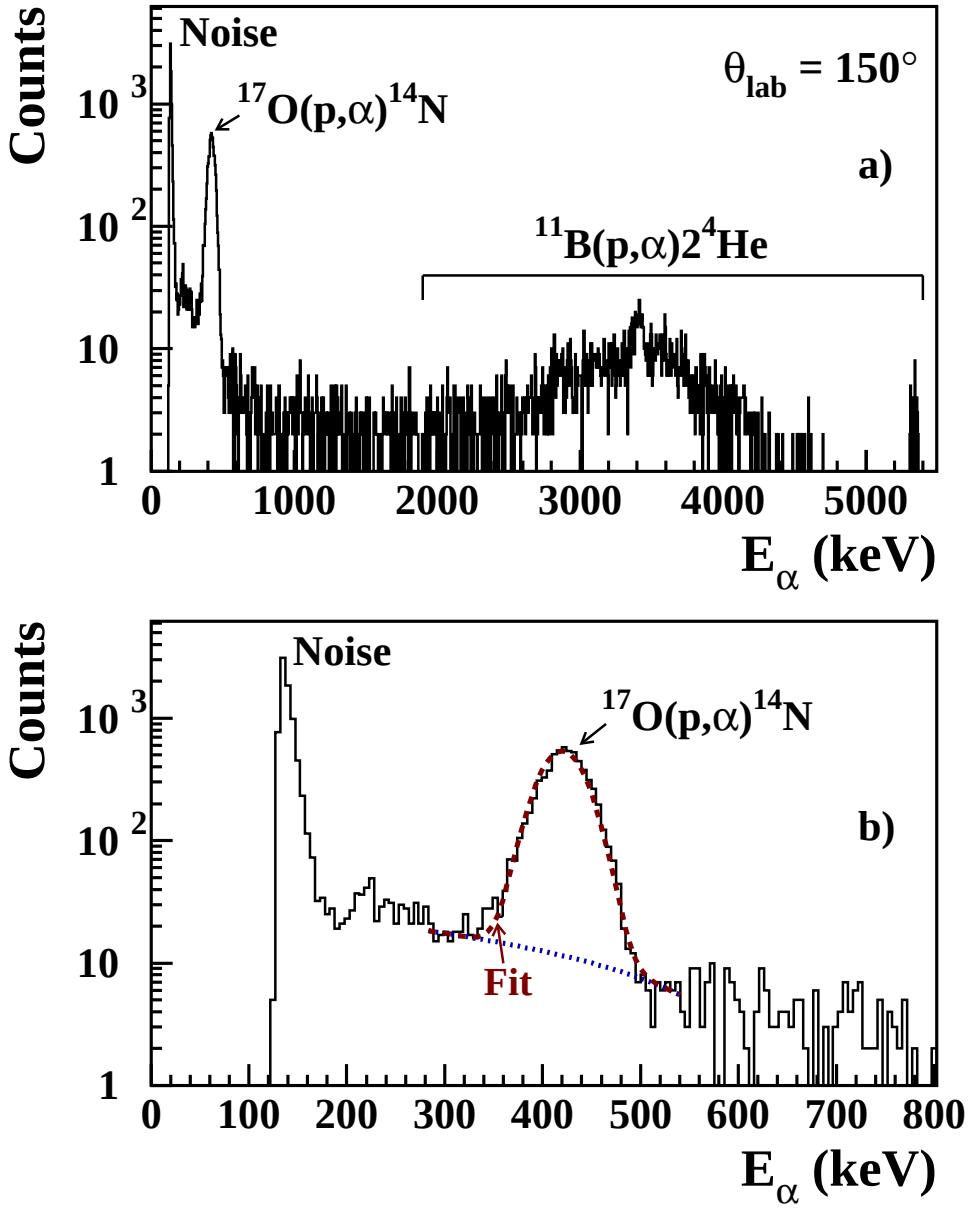

FIG. 4: (Color online) (a) Sample α spectrum obtained in the ^{17}O(p,α)^{14}N experiment with the detector at $\theta_{\rm lab}$=150°. The proton energy is $E_p^{\rm lab}$=196.5 keV and the accumulated charge is equal to 0.93 C. The broad peak labelled ^{11}B(p,α)2^{4}He is due to a slight contamination of boron in the used target. (b) Relevant part of the spectrum with a least-squares fit to the data points: dotted line – fitted linear background; dashed line – fitted Gaussian function with intensity, position and standard deviation as free parameters.

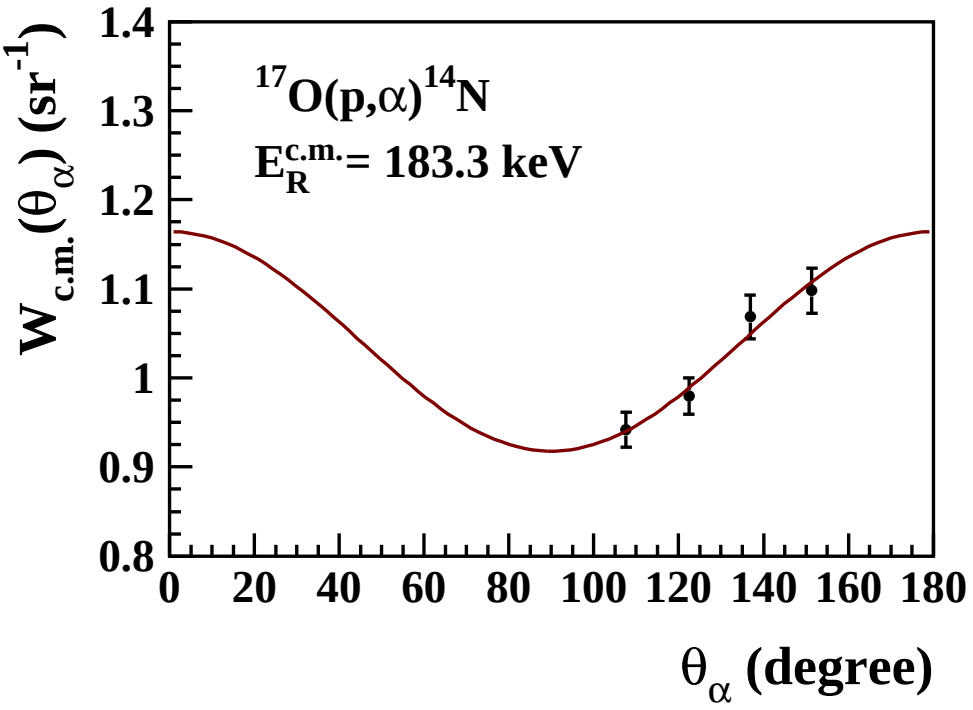

FIG. 5: (Color online) Angular distribution (center of mass) for the ^{17}O(p,α)^{14}N resonance at $E_{\rm c.m.}$=183.3 keV. The solid line shows a Legendre-polynomial fit to the data points, $W_{\rm c.m.}(\theta_\alpha) = 1 + a_2 P_2(\cos\theta_\alpha)$, which yields a_2=0.16±0.03.

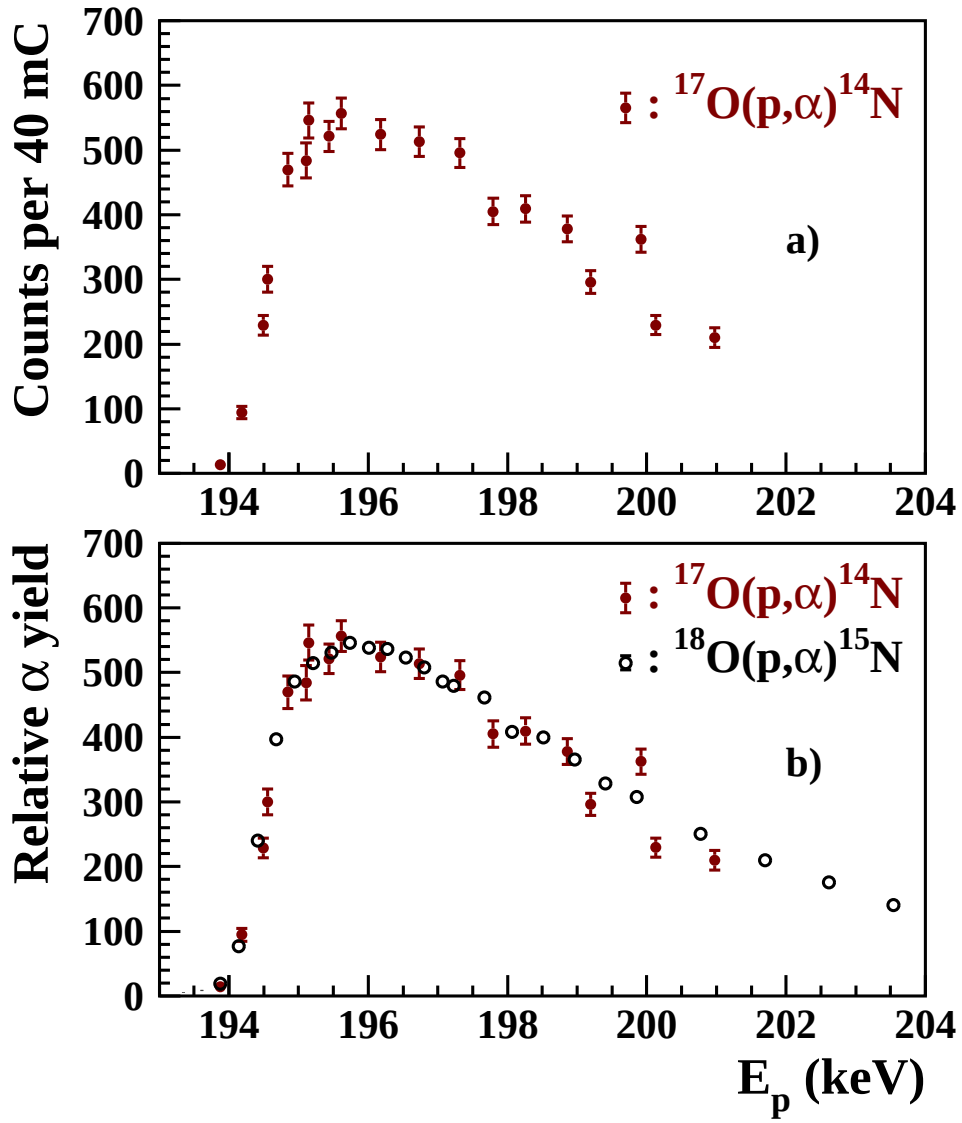

FIG. 6: (Color online) (a) Excitation function for the newly observed resonance at $E_R^{\rm lab}$=194.1 keV in the ^{17}O(p,α)^{14}N reaction. Yields are given by the sum of the number of counts observed in each of the four detectors normalized according to the measured angular distribution. (b) Comparison of excitation functions for the new resonance at $E_R^{\rm lab}$=194.1 keV in the ^{17}O(p,α)^{14}N reaction (filled symbols) and the well-known ^{18}O(p,α)^{15}N resonance at $E_R^{\rm lab}$=150.9 keV (empty symbols). The data for the latter resonance were appropriately normalized and shifted in energy to be compared with those obtained with the ^{17}O target.

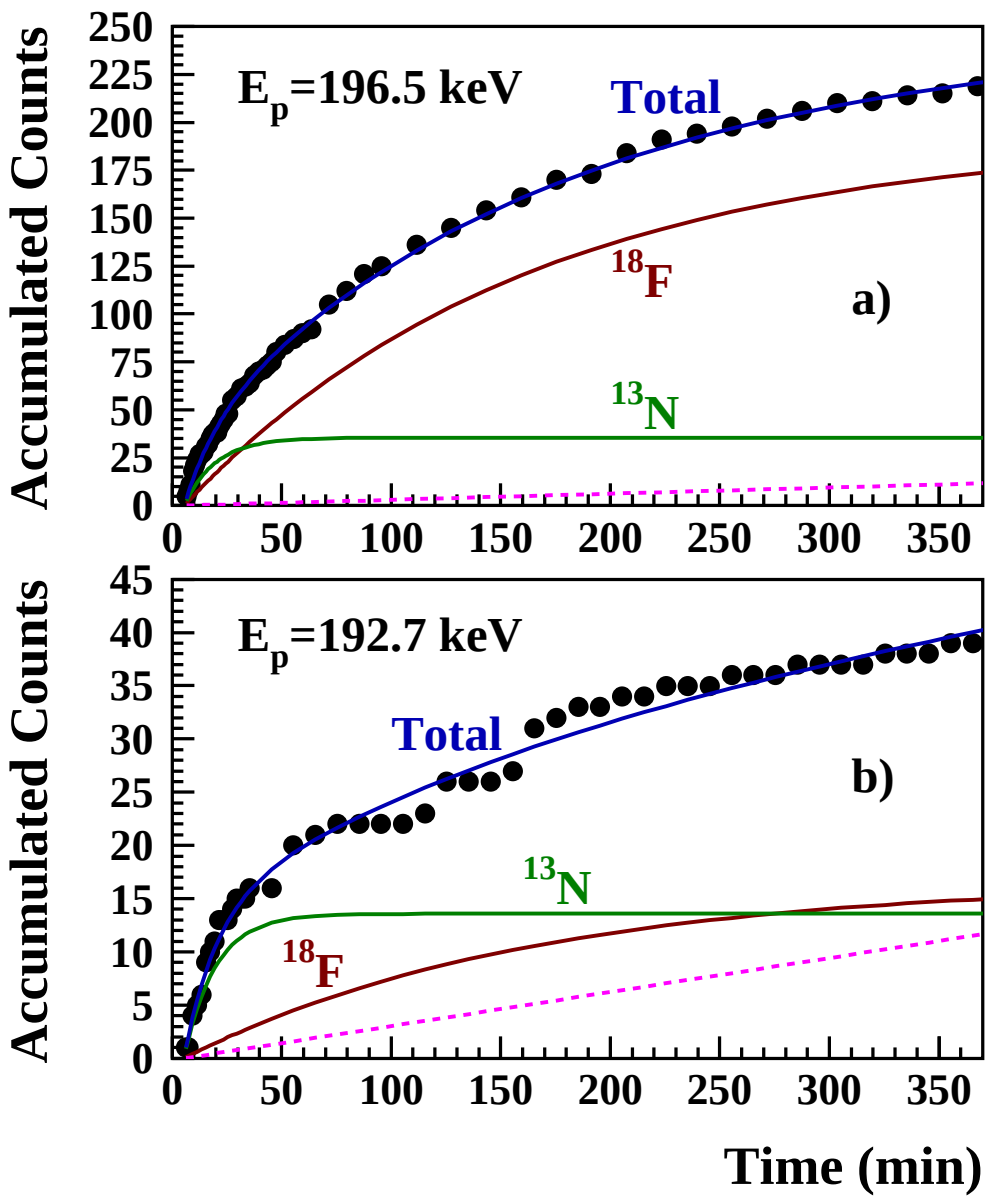

FIG. 7: (Color online) Measured β^+ activities of two ^{17}O-implanted targets irradiated at (a) $E_p^{\rm lab}$=196.5 keV (on-resonance) and (b) $E_p^{\rm lab}$=192.7 keV (off-resonance). The time origin corresponds to the stopping of the proton irradiation. Also shown are the fitted ^{18}F and ^{13}N decay curves (solid lines) and the measured background radiation (dashed lines).

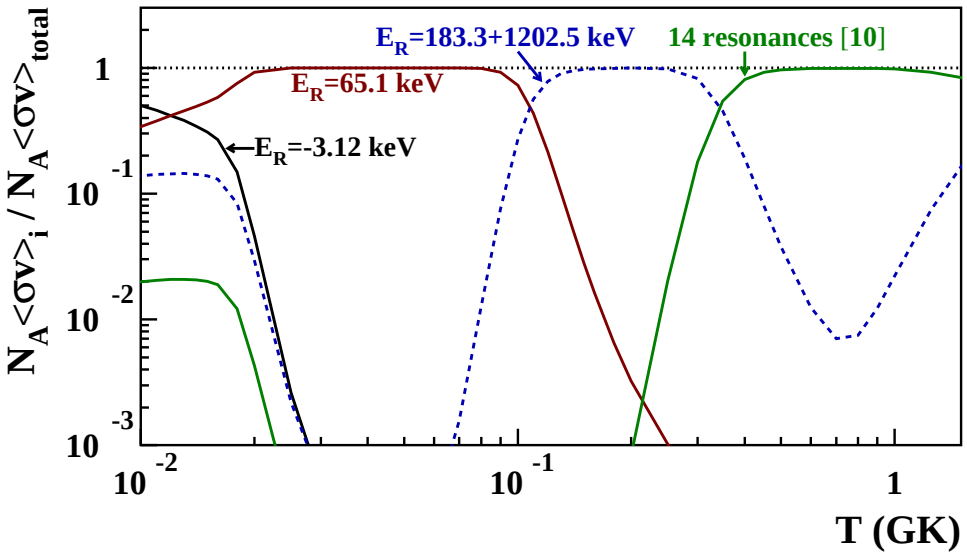

FIG. 8: (Color online) Ratios of individual reaction rate contributions to the total modal rate for the ^{17}O(p,α)^{14}N reaction. The unlabelled solid and dashed lines below 0.02 GK correspond to tail contributions of the resonances at 0.557+0.677 MeV and 1.202 MeV, respectively (see text).

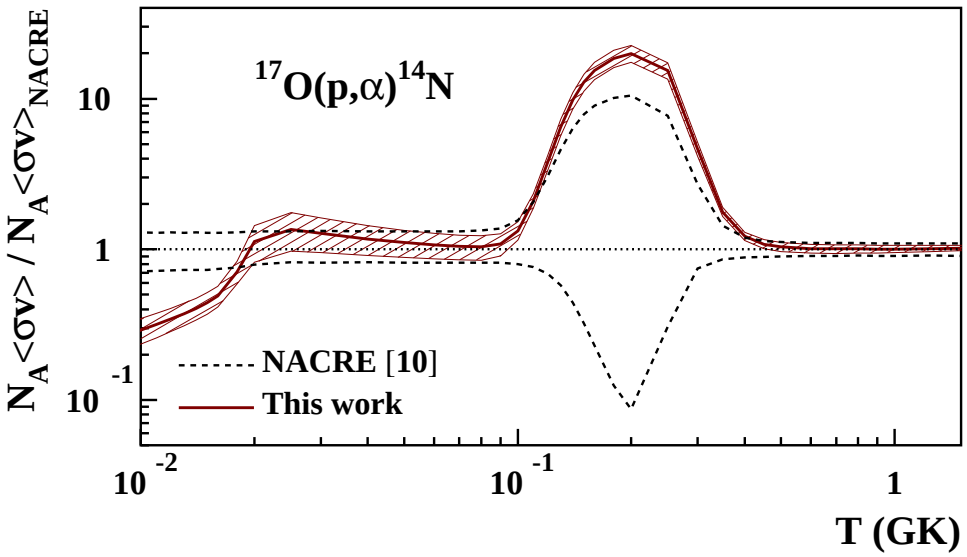

FIG. 9: (Color online) Ratio of present and previous [10] reaction rates for ^{17}O(p,α)^{14}N given as the solid line with hatched area representing uncertainties. The dashed lines indicate the previous [10] lower and upper limits for the total rate.

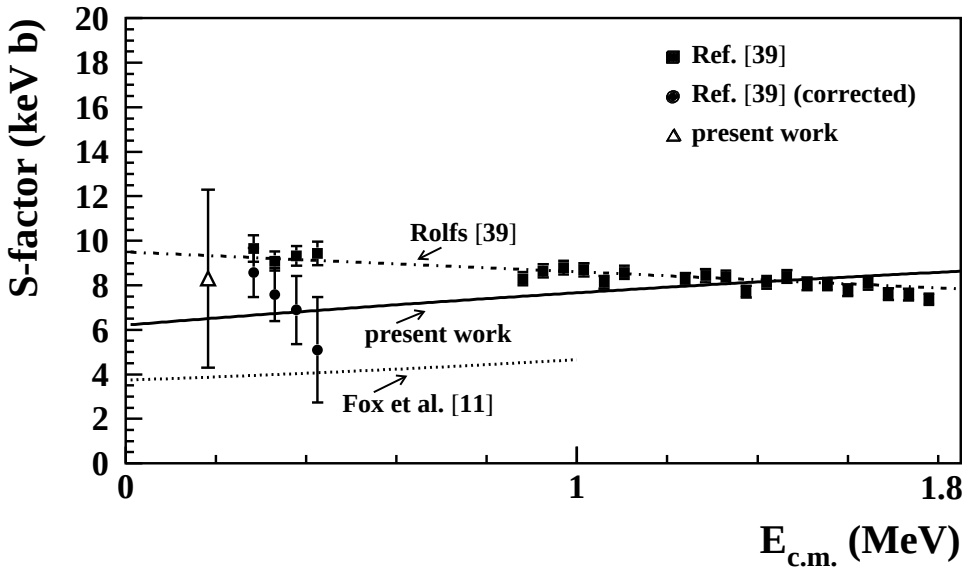

FIG. 10: Previous [11, 39] and present estimates of the direct capture S-factor in the ^{17}O(p,γ)^{18}F reaction for $E_{\rm c.m.}$=0–1.8 MeV. The data points are from Ref. [39] and the present work (triangle at $E_{\rm c.m.}$=180.2 keV). The four squares at low energy (<0.45 MeV) are original data from Ref. [39] and circles are corrected low-energy values (see text). The 19 data points above $E_{\rm c.m.}$=0.88 MeV are representative of the larger number of measured values, which cannot be accurately extracted from Fig. 17 of Ref. [39]. They were generated from a draw in a band around the best estimated value [39] of the DC S-factor (dot-dashed line) with a distribution (and error bars) in accordance with the data spread appreciated from Fig. 17 of Ref. [39]. The solid line shows the present calculations of the DC S-factor, whereas dot-dashed and dotted lines are the previous calculations from Refs. [39] and [11], respectively (see text). Note that the upturn of the S-factor at energies below 0.1 MeV visible in Fig. 17 of Ref. [39] has no influence on the fit and was not considered.

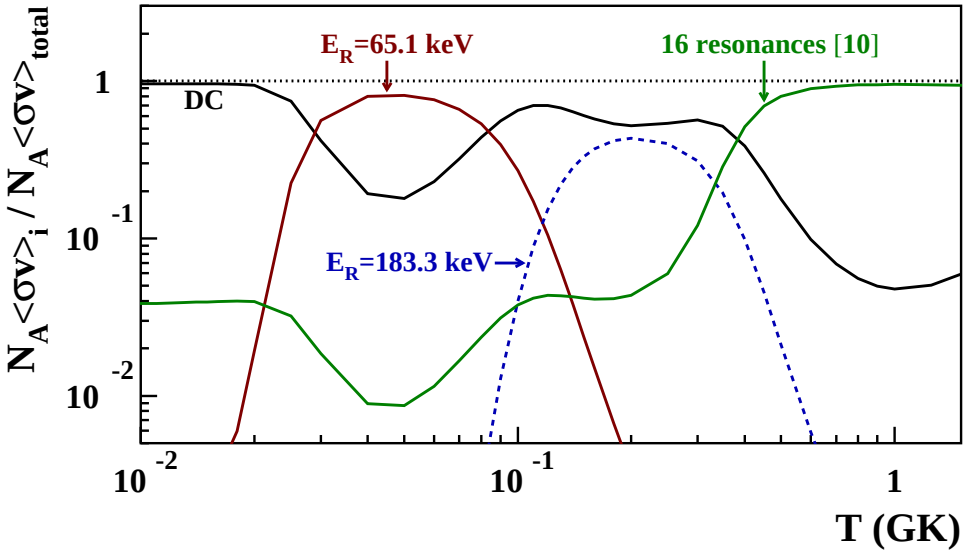

FIG. 11: (Color online) Ratios of individual reaction rate contributions to the total modal rate for the ^{17}O(p,γ)^{18}F reaction.

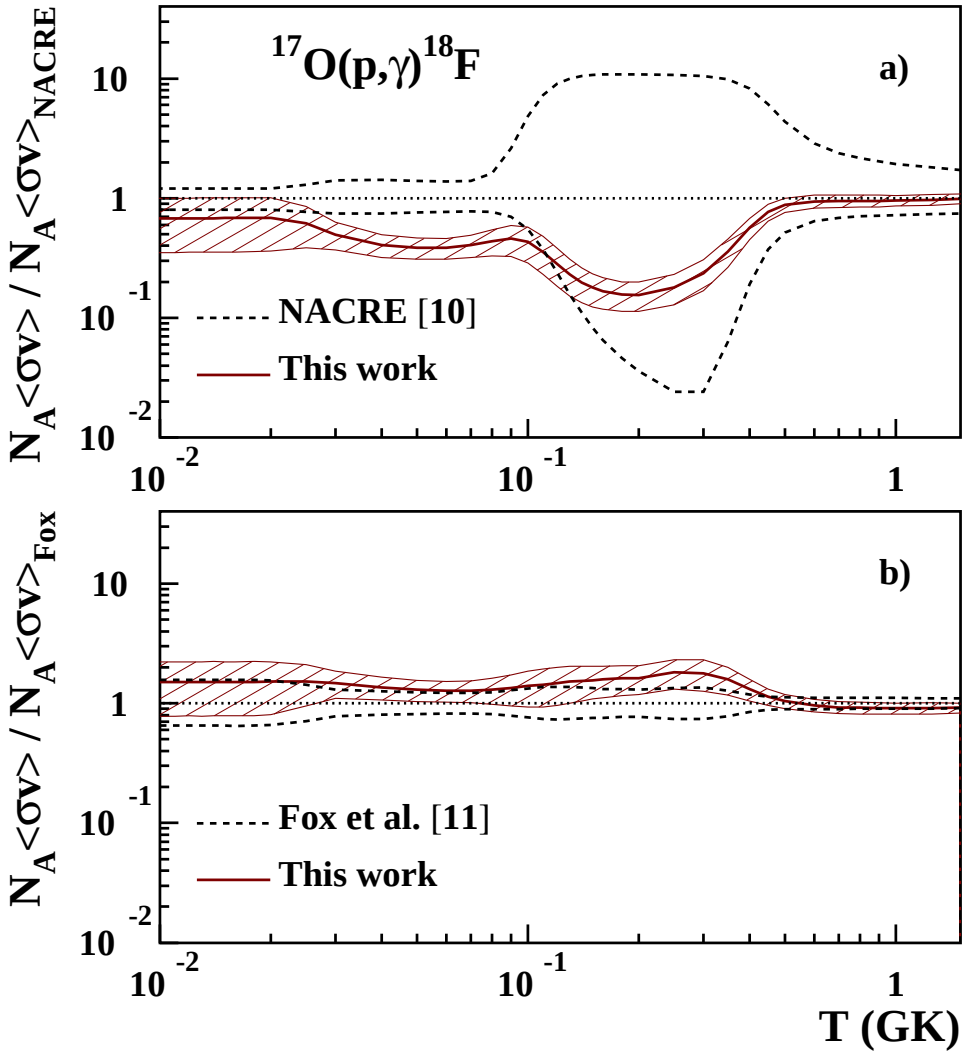

FIG. 12: (Color online) Comparison of present and previous reaction rates for the ^{17}O(p,γ)^{18}F reaction. In part a (b) is given the ratio of the present rates to the rates evaluated in Ref. [10] (Ref. [11]). The hatched area gives the present uncertainties in the reaction rates. Upper and lower limits for the rates of Refs. [10, 11] are given as dashed lines.